and propagation [3,35,36]. Our current study further demonstrates that the microtubule depolymerizing reagent, nocodazole, or the expression of microtubule-destabilizing protein stathmin, significantly inhibits the enhancement of HIV-1 particle production by SOCS1, suggesting a possible role of the microtubule network in regular HIV-1 particle production.

Our previous report indicated that the targeted depletion of SOCS1 results in the prominent perinuclear accumulations of HIV-1 Gag in 293T cells [11]. Our current study shows that nocodazole treatment or stathmin expression only slightly affects Gag release in non-SOCS1 overexpressing cells. This difference might be attributable to the following two possibilities. First, SOCS1 may affect Gag at multiple points during trafficking and assembly, and a critical point could be prior to the microtubule-mediated events that can be affected by nocodazole or stathmin. Second, there are multiple pathways to the delivery of exogenously expressed Gag protein from the cytoplasm to the plasma membrane in addition to microtubule-directed transport. Furthermore, we are currently uncertain whether the Gag association with microtubules is mediated by other microtubule binding proteins in cooperation with SOCS1, or whether SOCS1 directly associates with HIV-1 Gag on the microtubules. Further careful analysis must be performed to elucidate these possibilities.

Acknowledgements

We thank Drs. A. Yoshimura, Y. Tanaka, K.P. Lu and J.A. Komano for providing materials, and R. Kimura, S. Takahama and H. Soeda for their excellent technical assistance. This work was supported in part by grants from the Ministry of Education, Culture, Sports, Science and Technology of Japan (20390136, 13226027, 14406009 and 1941075) and Human Health Science (H19-001) to N.Y. and A.R.

References

[1] Sorin, M. and Kalpana, G.V. (2006) Dynamics of virus–host interplay in HIV-1 replication. Curr. HIV Res. 4, 117–130.
[2] Trkola, A. (2004) HIV-host interactions: vital to the virus and key to its inhibition. Curr. Opin. Microbiol. 7, 407–411.
[3] Naghavi, M.H. and Goff, S.P. (2007) Retroviral proteins that interact with the host cell cytoskeleton. Curr. Opin. Immunol. 19, 402–407.
[4] Lama, J. and Planelles, V. (2007) Retrovirology 4, 52.
[5] Dong, X. et al. (2005) AP-3 directs the intracellular trafficking of HIV-1 Gag and plays a key role in particle assembly. Cell 120, 663–674.
[6] Perlman, M. and Resh, M.D. (2006) Identification of an intracellular trafficking and assembly pathway for HIV-1 gag. Traffic 7, 731–745.
[7] Alroy, I. et al. (2005) The trans-Golgi network-associated human ubiquitin-protein ligase POSH is essential for HIV type 1 production. Proc. Natl. Acad. Sci. USA 102, 1478–1483.
[8] Barr, S.D., Smiley, J.R. and Bushman, F.D. (2008) The interferon response inhibits HIV particle production by induction of TRIM22. PLoS Pathog. 4, e1000007.
[9] Joshi, A., Garg, H., Nagashima, K., Bonifacino, J.S. and Freed, E.O. (2008) GGA and Arf proteins modulate retrovirus assembly and release. Mol. Cell 30, 227–238.
[10] Ono, A., Ablan, S.D., Lockett, S.J., Nagashima, K. and Freed, E.O. (2004) Phosphatidylinositol (4, 5) bisphosphate regulates HIV-1 Gag targeting to the plasma membrane. Proc. Natl. Acad. Sci. USA 101, 14889–14894.
[11] Ryo, A. et al. (2008) SOCS1 is an inducible host factor during HIV-1 infection and regulates the intracellular trafficking and stability of HIV-1 Gag. Proc. Natl. Acad. Sci. USA 105, 294–299.
[12] Ryo, A. et al. (2003) Regulation of NF-kappaB signaling by Pin1-dependent prolyl isomerization and ubiquitin-mediated proteolysis of p65/RelA. Mol. Cell 12, 1413–1426.
[13] Wagner, R., Graf, M., Bieler, K., Wolf, H., Grunwald, T., Foley, P. and Uberla, K. (2000) Rev-independent expression of synthetic gag-pol genes of human immunodeficiency virus type 1 and simian immunodeficiency virus: implications for the safety of lentiviral vectors. Hum. Gene Ther. 11, 2403–2413.
[14] Stang, E., Blystad, F.D., Kazazic, M., Bertelsen, V., Brodahl, T., Raiborg, C., Stenmark, H. and Madshus, I.H. (2004) Cbl-dependent ubiquitination is required for progression of EGF receptors into clathrin-coated pits. Mol. Biol. Cell 15, 3591–3604.
[15] Sawasaki, T., Ogasawara, T., Morishita, R. and Endo, Y. (2002) A cell-free protein synthesis system for high-throughput proteomics. Proc. Natl. Acad. Sci. USA 99, 14652–14657.
[16] Vuong, B.Q. et al. (2004) SOCS-1 localizes to the microtubule organizing complex-associated 20S proteasome. Mol. Cell Biol. 24, 9092–9101.
[17] Westermann, S. and Weber, K. (2003) Post-translational modifications regulate microtubule function. Nat. Rev. Mol. Cell Biol. 4, 938–947.
[18] Kobayashi, T. and Yoshimura, A. (2005) Keeping DCs awake by putting SOCS1 to sleep. Trends Immunol. 26, 177–179.
[19] Kile, B.T., Schulman, B.A., Alexander, W.S., Nicola, N.A., Martin, H.M. and Hilton, D.J. (2002) The SOCS box: a tale of destruction and degradation. Trends Biochem. Sci. 27, 235–241.
[20] Jager, S., Gottwein, E. and Krausslich, H.G. (2007) Ubiquitination of human immunodeficiency virus type 1 Gag is highly dependent on Gag membrane association. J. Virol. 81, 9193–9201.
[21] Strack, B., Calistri, A., Accola, M.A., Palu, G. and Gottlinger, H.G. (2000) A role for ubiquitin ligase recruitment in retrovirus release. Proc. Natl. Acad. Sci. USA 97, 13063–13068.
[22] Naka, T. et al. (1997) Structure and function of a new STAT-induced STAT inhibitor. Nature 387, 924–929.
[23] Endo, T.A. et al. (1997) A new protein containing an SH2 domain that inhibits JAK kinases. Nature 387, 921–924.
[24] Starr, R. et al. (1997) A family of cytokine-inducible inhibitors of signalling. Nature 387, 917–921.
[25] Poole, E., Strappe, P., Mok, H.P., Hicks, R. and Lever, A.M. (2005) HIV-1 Gag-RNA interaction occurs at a perinuclear/centrosomal site; analysis by confocal microscopy and FRET. Traffic 6, 741–755.
[26] Greber, U.F. and Way, M. (2006) A superhighway to virus infection. Cell 124, 741–754.
[27] Benboudjema, L., Mulvey, M., Gao, Y., Pimplikar, S.W. and Mohr, I. (2003) Association of the herpes simplex virus type 1 Us11 gene product with the cellular kinesin light-chain-related protein PAT1 results in the redistribution of both polypeptides. J. Virol. 77, 9192–9203.
[28] Dohner, K. and Sodeik, B. (2005) The role of the cytoskeleton during viral infection. Curr. Top. Microbiol. Immunol. 285, 67–108.
[29] Jouvenet, N., Monaghan, P., Way, M. and Wileman, T. (2004) Transport of African swine fever virus from assembly sites to the plasma membrane is dependent on microtubules and conventional kinesin. J. Virol. 78, 7990–8001.
[30] Leblanc, J.J., Perez, O. and Hope, T.J. (2008) Probing the structural states of human immunodeficiency virus type 1 pr55gag by using monoclonal antibodies. J. Virol. 82, 2570–2574.
[31] Tang, Y., Winkler, U., Freed, E.O., Torrey, T.A., Kim, W., Li, H., Goff, S.P. and Morse 3rd, H.C. (1999) Cellular motor protein KIF-4 associates with retroviral Gag. J. Virol. 73, 10508–10513.
[32] Martinez, N.W., Xue, X., Berro, R.G., Kreitzer, G. and Resh, M.D. (2008) Kinesin KIF4 regulates intracellular trafficking and stability of the human immunodeficiency virus type 1 Gag polyprotein. J. Virol. 82, 9937–9950.
[33] Finzi, A., Orthwein, A., Mercier, J. and Cohen, E.A. (2007) Productive human immunodeficiency virus type 1 assembly takes place at the plasma membrane. J.Virol. 81, 7476–7490.
[34] Jouvenet, N., Neil, S.J., Bess, C., Johnson, M.C., Virgen, C.A., Simon, S.M. and Bieniasz, P.D. (2006) Plasma membrane is the site of productive HIV-1 particle assembly. PLoS Biol. 4, e435.
[35] Jolly, C., Mitar, I. and Sattentau, Q.J. (2007) Requirement for an intact T-cell actin and tubulin cytoskeleton for efficient assembly and spread of human immunodeficiency virus type 1. J. Virol. 81, 5547–5560.
[36] Handley, M.A., Paddock, S., Dall, A. and Panganiban, A.T. (2001) Association of Vpu-binding protein with microtubules and Vpu-dependent redistribution of HIV-1 Gag protein. Virology 291, 198–207.

 DOI 10.1002/eji.200939433 Eur. J. Immunol. 2009. 39: 2822–2830

European Journal of Immunology

Concurrent infection with *Heligmosomoides polygyrus* suppresses anti-*Plasmodium yoelii* protection partially by induction of $CD4^+CD25^+Foxp3^+$ Treg in mice

Kohhei Tetsutani[1], Kenji Ishiwata[2], Hidekazu Ishida[1], Liping Tu[1], Motomi Torii[3], Shinjiro Hamano[1,4], Kunisuke Himeno[1] and Hajime Hisaeda[1]

[1] Department of Parasitology, Kyushu University Graduate School of Medical Science, Fukuoka, Japan
[2] Department of Tropical Medicine, The Jikei University School of Medicine, Tokyo, Japan
[3] Department of Molecular Parasitology, Ehime University School of Medicine, Ehime, Japan
[4] Department of Parasitology, Institute of Tropical Medicine (NEKKEN) and the Global COE program, Nagasaki University, Nagasaki, Japan

Malaria and intestinal nematode infection are widespread and co-infection frequently occurs. We investigated whether co-infected intestinal nematodes modulate immunity against co-existing malaria parasites. Infection of C57BL/6 mice with *Plasmodium yoelii* 17XNL (Py) was transient and self-limiting, but preceding infection with *Heligmosomoides polygyrus* (Hp), a mouse intestinal nematode, exacerbated malaria resulting in higher parasite burdens and poor survival of the mice. Co-infection with Hp led to reduced Py-responsive proliferation and IFN-γ production of spleen cells, and higher activation of $CD4^+CD25^+Foxp3^+$ Treg. *In vivo* depletion of Treg recovered anti-Py immunity and rescued co-infected mice from exacerbated malaria. However, we did not observe any obvious *ex vivo* activation of Treg by either Hp products or living worms. Our results suggest that intestinal nematodes moderate host immune responses during acute malaria infection by aggressive activation of Treg. Elucidation of the mechanisms of Treg activation *in situ* is a target for future analyses.

Key words: Adaptive immunity · Malaria · Intestinal nematode · Regulatory T cell

Introduction

Malaria is the most widespread and deadliest parasitic disease, and it causes hundreds of millions of clinical cases and millions of deaths annually worldwide. The severity of the disease is strongly related to the malaria parasite species, parasite density and immune responses of the host. Protective immunity against malaria develops very slowly, and individuals living in endemic areas suffer from repeated infections. The major reason why immunity to malaria is difficult to develop is that malaria parasites effectively evade host immunity in several ways. Antigenic diversity/variation allows parasites to escape immune recognition [1, 2]. They also actively suppress immunity *via* induction of Treg [3, 4], effector T-cell apoptosis [5] or dysfunctions of APCs [6]. These immune evasion mechanisms also make it difficult to develop effective vaccines against malaria.

Environmental factors, such as exposure to infective vectors [7], nutritional status [8], medical/public health interventions [9] and concurrent infections with other pathogens [10], also affect the outcome of the disease. Among infections, chronic but mostly asymptomatic infection with intestinal helminths is the most

Correspondence: Dr. Kohhei Tetsutani
e-mail: tetztani@gmail.com

prevalent in malarial areas [11, 12] (http://gamapserver.who.int/mapLibrary/Files/Maps/global_cases.jpg, http://www.who.int/intestinal_worms/epidemiology/map/en/index.html) and the population in a given area tends to suffer from both infections. Generally, as well as schistosomes [13] or filarias [14], intestinal helminths are known to modulate, and mainly suppress, host immune responses [15]. Indeed, studies in Thailand showed that infection with intestinal helminths increased the frequency of malaria episodes, but decreased malaria-associated serious inflammations, such as cerebral malaria, acute renal failure or pulmonary edema [16, 17]. These observations suggest that intestinal helminths suppress host responses of both protective immunity and inflammation during malaria infection. Therefore, it is important to understand the relationship between co-infection and host immune responses for effective control of malaria.

Several researchers have studied the effects of co-infection with intestinal helminths on the course of malaria using mouse models and reported that co-infection causes rapid growth of malaria parasites *in vivo* [18–20]. A good experimental model is the mouse intestinal nematode *Heligmosomoides polygyrus* (Hp), which resides in the upper small intestine for a long time and is known to modulate host responses through various mechanisms [21, 22]. Su *et al.* [18] described that proliferation of immune cells in response to the malaria Ag or production of anti-malaria Ab was suppressed with the induction of regulatory cytokines during co-infection with Hp and *Plasmodium chabaudi*. Unlike the results from human studies in Thailand, Hp did not attenuate inflammation-associated experimental cerebral malaria, but it did suppress anti-parasite immunity during infection with *P. berghei* ANKA [20]. These observations are compatible with our findings from studies on mice infected with Hp [21]. However, the interactions between nematodes inside the intestine and immune systems are still not well understood.

Here, we examined the effects of co-infection with Hp on the course of infection with the rodent malaria parasite *P. yoelii* 17XNL (Py) by focusing on $CD4^+CD25^+Foxp3^+$ Treg as key factors linking nematodes and suppressed host protection. We found that Hp and Py co-infection induced strongly activated Treg, which suppressed anti-Py effector mechanisms, increased malaria parasite growth *in vivo* and deteriorated survival of mice.

Results

Preceding infection with Hp deteriorates Py infection

First, we infected Hp-harboring mice with the non-lethal malaria strain Py. As previously reported [4], infection with Py alone exhibited transient elevation of parasitemia and a spontaneous cure within 3–4 wk (Fig. 1A). Co-infection with Hp caused rapid growth of Py at the early and late phases of infection (Fig. 1A), and all the mice died (Fig. 1B). Unlike the rodent parasite *P. berghei*, Py is widely considered not to induce fatal host-damaging inflammations, such as liver injury [23]. Therefore, the cause of death of the co-infected mice was supposed to be failure to eradicate the parasites, suggesting that the presence of Hp suppressed host immune responses against Py.

Co-infection with Hp suppresses adaptive immune responses against Py

Next, we analyzed the immune responses to Py in Hp-harboring mice after infection with Py. Splenocytes isolated from co-infected mice were stimulated with Py-parasitized RBC (pRBC) and analyzed for their proliferative responses (Fig. 2A). Whole spleen cells from mice infected with Py alone showed remarkable proliferation in response to pRBC. However, preceding infection with Hp significantly suppressed this proliferation. Similar results were obtained when $CD4^+CD25^-$ spleen cells were examined. The suppression was not specific for Py Ag because responses to ConA were also suppressed. We also analyzed production of IFN-γ, one of the indispensable effector molecules against malaria parasites [24]. Consistent with the proliferative responses, production of IFN-γ by spleen cells of mice infected

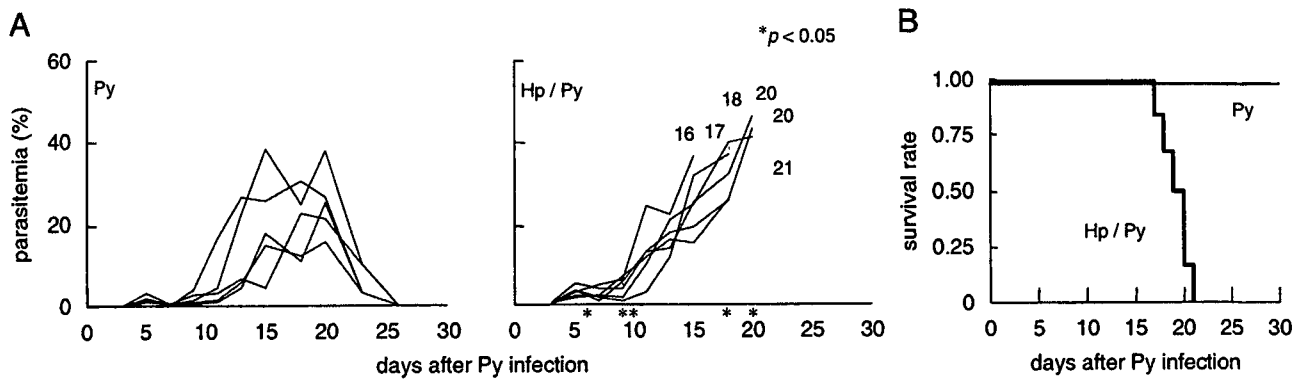

Figure 1. *H. polygyrus* and *P. yoelii* NL co-infection in C57BL/6N male mice. Mice ($n = 5$–7) were infected with Hp larvae orally and then i.p. infected with Py pRBC (2.5×10^4 cells/mouse) 2 wk later. Parasitemia (A) and survival (B) of the mice were monitored daily. Each line shows the parasitemia curve of an individual mouse, and the numbers show the death day of each individual (A). Parasitemia was analyzed statistically by Student's t-test. Asterisks show significant differences at the indicated p value. The experiment was repeated three times with similar results.

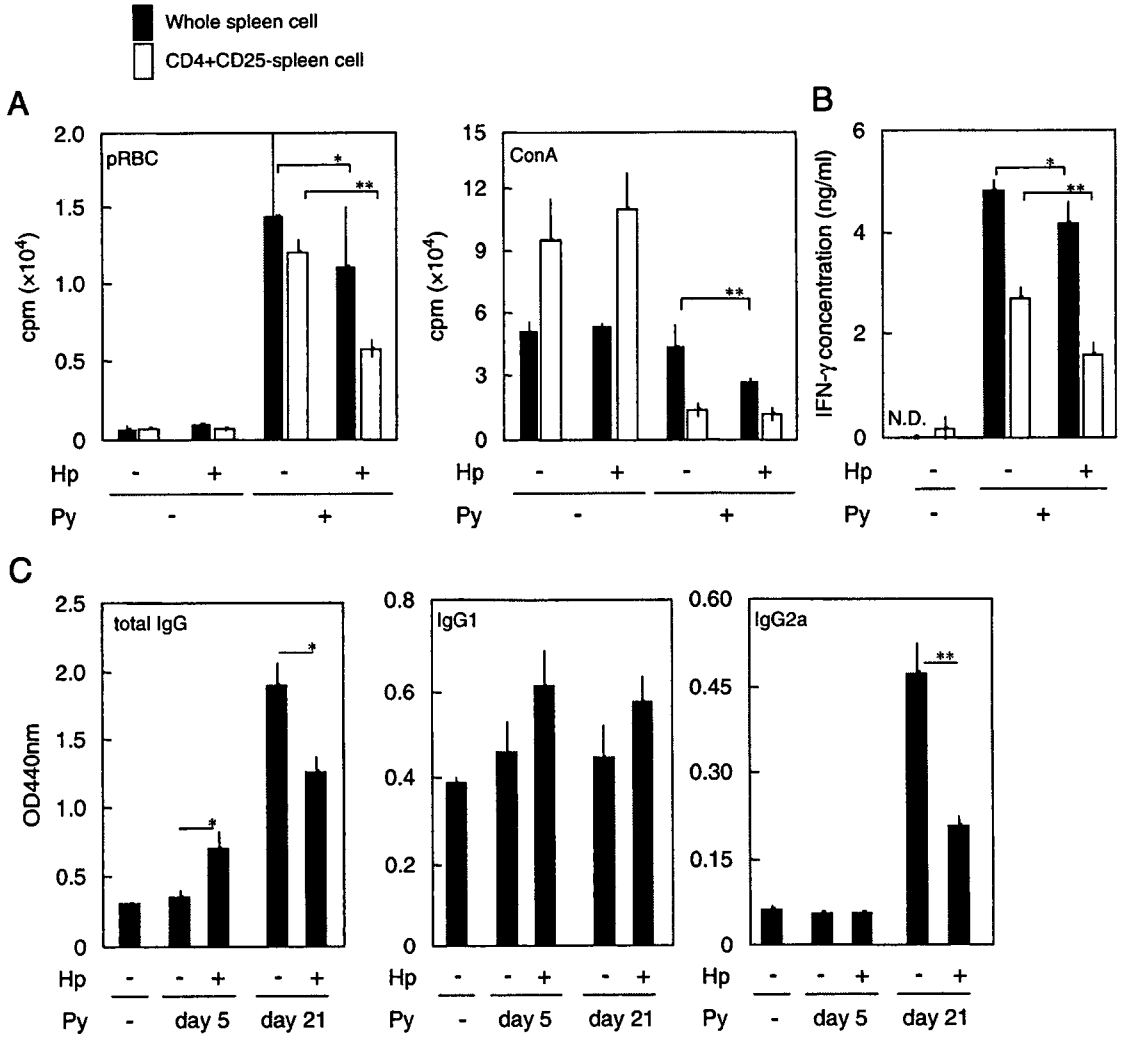

Figure 2. Effects of co-infection with Hp on immune responses against Py. Spleen cells or $CD4^+CD25^-$ spleen cells were isolated from mice co-infected with Hp and Py at 5 days after Py infection. Whole spleen cells (2×10^5; closed bars) or $CD4^+CD25^-$ cells (1×10^5) and $CD11c^+$ cells (1×10^4) from uninfected mice (open bars) were cultured with pRBC (2×10^5) or ConA (2.5 μg/mL). (A) Proliferation was analyzed by ^{3}H-thymidine uptake. (B) IFN-γ concentrations in the culture supernatants with pRBC were measured by ELISA. (C) Anti-Py IgG, IgG1 or IgG2a Ab in sera taken at the indicated days after Py infection were measured by ELISA using Py Ag. (D) $CD11c^+$ cells (1×10^4) were isolated from mice co-infected with Hp and Py at 5 days after Py infection and cultured with $CD4^+CD25^-$ cells (1×10^5) from Py-infected mice and pRBC (2×10^5). Proliferation was analyzed by ^{3}H-thymidine uptake. Data represent the means ±SE of triplicate samples in a representative of 3–6 repeated experiments. $^*p<0.05$, $^{**}p<0.01$; between the samples linked with horizontal lines, Student's t-test.

with Py was significantly suppressed by preceding infection with Hp (Fig. 2B). These results clearly indicate that co-infection with Hp suppresses cellular immune responses. Humoral immunity, represented by IgG specific for malaria parasites, was subsequently analyzed (Fig. 2C). Infection with Py alone led to the development of IgG2a-dominant Ab responses at 21 days after infection, but had no effect at 5 days after infection. Despite the higher parasitemia at the early phase, co-infection with Hp rather enhanced the production of IgG1. Conversely, it remarkably reduced the production of IgG2a in curable mice singly infected with Py, suggesting that the Ab responsible for protection at the late phase may be IgG2a. These results demonstrate that the increased Py parasitemia at the early stage of infection is due to suppression of cellular responses, rather than Ab responses. Therefore, we subsequently focused on the suppression of cellular responses at the early phase.

Co-infection with Hp and Py induces aggressively suppressive Treg

In a previous report, we demonstrated that activation of Treg occurs during infection with a lethal strain of *P. yoelii* [4]. In addition, it has been reported that the functions of Treg are altered in mice infected with Hp [25]. These observations led us to analyze the Treg behaviors in co-infected mice. As early as 5 days after infection with Py, the proportion of $CD4^+CD25^+$ $Foxp3^+$ cells was increased in the spleen, as well as MFI of either

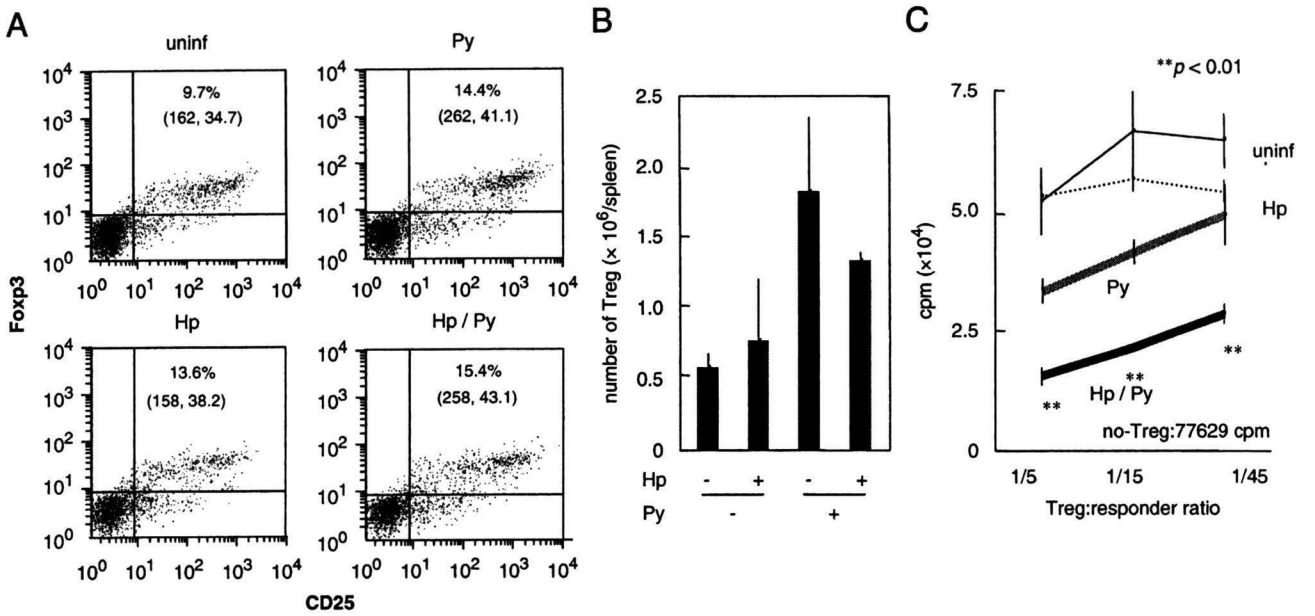

Figure 3. $CD4^+CD25^+Foxp3^+$ cells in Hp+Py co-infection. Spleen cells stained with fluorochrome-conjugated anti-CD4, anti-CD25 and anti-Foxp3 Ab were analyzed by flow cytometry at 5 days after infection with Py. (A) The dot plots represent the expression levels of CD25 and Foxp3 in CD4-gated cells from the indicated mice. Percentage inside of each plot shows the frequency of $CD4^+CD25^+Foxp3^+$ cells in total $CD4^+$ cells. The number inside of brackets shows the mean fluorescent intensity of CD25 (left) and Foxp3 (right). (B) The $CD4^+CD25^+Foxp3^+$ cell populations in individual spleens were calculated. (C) The suppressive functions of Treg from co-infected mice were analyzed at 5 days after infection with Py. Splenic Treg from the indicated mice were cultured with $CD4^+CD25^-$ cells (1×10^5) as responders and $CD11c^+$ cells (1×10^4) obtained from the spleens of uninfected mice in the presence of ConA (2.5 μg/mL) at the indicated frequencies. The proliferation of responders was analyzed by ^3H-thymidine uptake. Data are presented as the means ±SE of three samples in a representative of three repeated experiments. Asterisks show significant differences by Student's t-test between Treg from Py-infected and Hp+Py-infected mice at the indicated p value.

CD25 or Foxp3 (Fig. 3A). The absolute number of $CD4^+CD25^+$ $Foxp3^+$ cells in individual spleens, calculated from the cell frequency by flow cytometry, was also increased (Fig. 3B). The amount of Foxp3 expressed in Treg may influence their functions [26], suggesting that Treg with the higher Foxp3 MFI observed in co-infection may have enhanced suppressive function. Thus, the suppressive function of Treg was determined by analyzing the degree of suppression of TCR-triggered T-cell proliferation at this time point. Co-infection with Hp enhanced the suppressive activity of Treg, but did not affect the number of Treg (Fig. 3B, C). These results suggest that co-infection with Hp and Py induces Treg more aggressively than single infection with Py, resulting in deteriorated malaria infection associated with suppressed cellular responses against Py.

In vivo depletion of Treg partially abolishes the suppressed protection against Py

To confirm that induction of Treg in mice co-infected with Hp and Py is responsible for the deteriorated infection with Py, we depleted Treg by i.p. application of an anti-CD25 Ab. This treatment depleted 85% of the $CD4^+CD25^+Foxp3^+$ Treg in the spleen, as evaluated by Foxp3 intracellular flow cytometry, at 5 days after infection (Fig. 4A). However, the depletion effect was transient and Treg were detected in mice treated with the anti-CD25 Ab at similarly high levels to those in control mice at 2 wk after the treatment (data not shown). As previously shown, infection with Py was self-limiting, and again mice co-infected with Hp suffered from higher parasitemia and finally succumbed to infection with Py (Fig. 4B, C). Depletion of Treg significantly decreased the parasitemia at the early phase of infection in co-infected mice. Furthermore, 40% of the co-infected mice depleted of Treg were able to limit the parasitemia and they survived (Fig. 4B, C).

The anti-malarial effector mechanisms were altered by depletion of Treg. The suppression of IFN-γ production by splenic $CD4^+$ T cells in response to pRBC observed in co-infected mice was clearly reversed after removal of Treg (Fig. 4D). Alterations in Ab responses due to co-infection with Hp, namely suppression of IgG and IgG2a at the later phase and enhancement of IgG at the early phase, were all offset by the removal of Treg (Fig. 4E). These results suggest that the deteriorated malaria infection in mice co-infected with Hp and Py was partially due to aggressive activation of Treg.

Hp worm products and living worms do not directly activate Treg *in vitro*

The preceding existence of Hp activates Treg in terms of enhanced suppressive functions during infection with Py. To investigate how co-infection with Hp induces stronger Treg, we performed *in vitro* Treg activation assays using various Hp products. Splenic Treg from Py-infected mice were stimulated

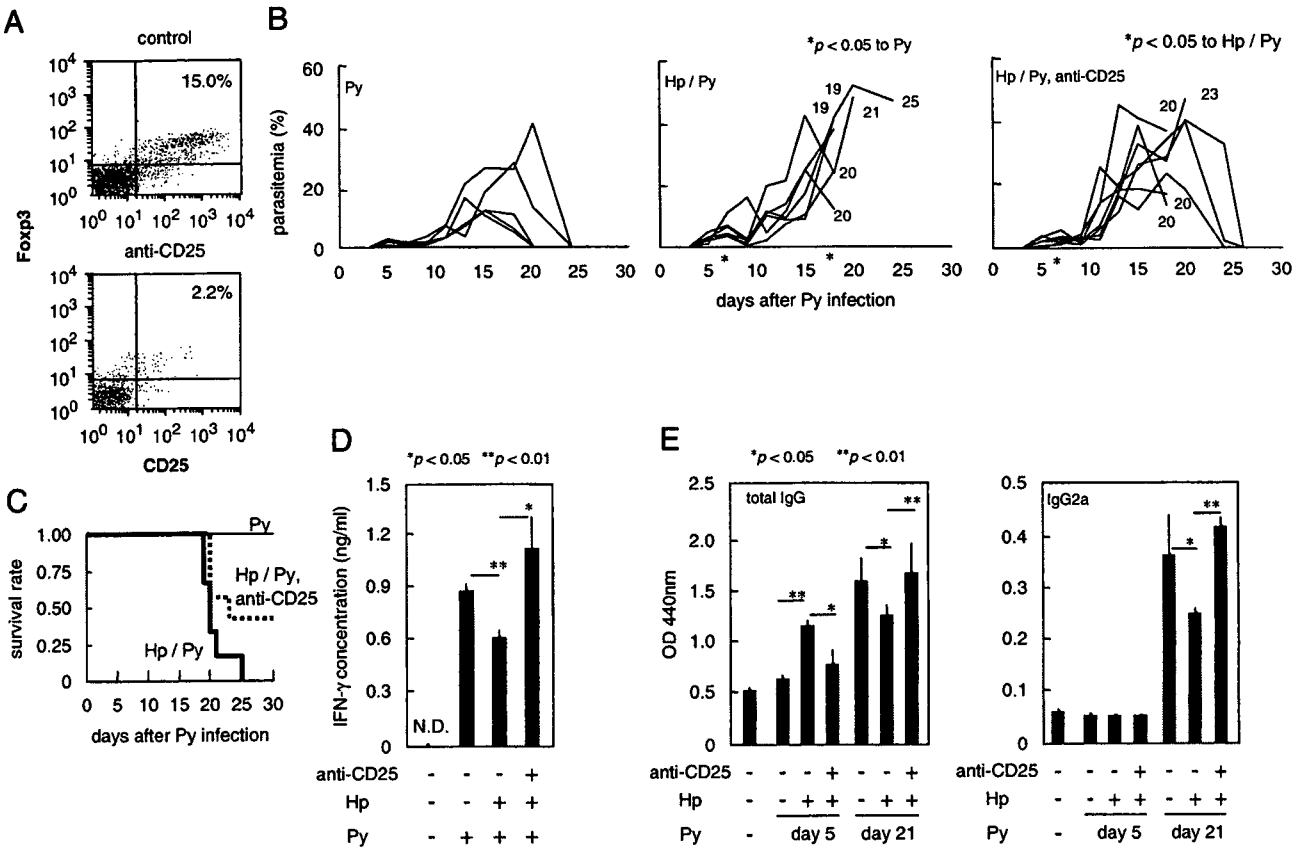

Figure 4. Effects of depletion of Treg in mice co-infected with Hp and Py. Spleen cells from mice depleted of Treg were analyzed as described in the legend for Fig. 3A. (A) The treatment depleted 85% of Treg in the spleen, as evaluated by flow cytometry on day 5 after Py infection. (B,C) Py infection in mice with or without depletion of Treg was monitored by the parasitemia (B) and survival (C) as described in the legend for Fig. 1. The infection experiments were repeated three times with similar results. (D, E) Immune responses and IFN-γ production in $CD4^+$ cells in response to pRBC (D) and serum levels of anti-Py IgG (E) were analyzed as described in the legend for Fig. 2. Data are presented as the means ±SE of three samples in a representative of 3–6 repeated experiments. Asterisks show significant differences at the indicated *p* values by Student's *t*-test.

with excretory/secretory (ES) Ag of Hp, an extract of adult Hp worms or living Hp worms in the presence of $CD11c^+$ DCs (Fig. 5). The cultured Treg were then analyzed for their suppressive activities. Treg cultured with medium alone still exhibited suppressive functions, although their effects were lower than those of freshly isolated Treg. However, none of the stimulatory conditions changed the suppressive abilities of the cultured Treg. The same tendency was observed when Treg were cultured without DC (data not shown) and when Treg from uninfected mice were stimulated with Hp preparations in combination with DC and pRBC, as well as without DC (data not shown). These results indicate that Hp worms residing in the intestine do not directly activate Treg.

Discussion

In the present study, we have demonstrated that a mouse intestinal nematode, Hp, was able to suppress anti-malaria protection *via* induction of Treg. Infection with malaria parasites is already known to activate Treg in humans and experimental models [3, 4], which allows rapid growth of malaria parasites. As previously reported [4], the non-lethal malaria parasite Py used in the present study does not strongly activate Treg and its low pathogenicity/virulence is closely linked to its failure to activate Treg. Therefore, it seems likely that activation of Treg in the presence of Hp converted the pathogenic behaviors of Py, as observed for a highly virulent *P. yoelii* strain [4]. Furthermore, the involvement of Treg activation for conversion to high virulence was clearly confirmed by the partial reversal of high parasitemia and mortality in mice depleted of Treg.

However, anti-CD25 treatment did not rescue all of the co-infected mice, partially because the depletion of Treg did not last longer than 2 wk. This finding may be supported by a previous observation that anti-CD25 treatment is insufficient because of a rapid expansion of Treg after infection with *P. yoelii* [27]. Interestingly, depletion of Treg recovered the suppression of presumably protective IgG responses at the late phase when Treg themselves reappeared comparably with the control Treg-sufficient mice. Therefore, besides activation of Treg, we cannot exclude various mechanisms supposed to cause the global immune suppression by intestinal helminths, regardless of the importance of Treg. For instance, the elevation of IgG1 observed at the early phase of infection suggests that Th2

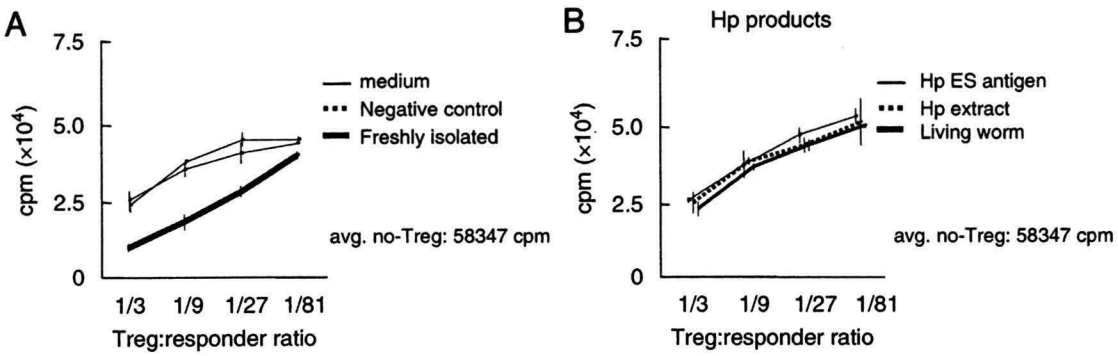

Figure 5. Stimulation of Treg with Hp products or living Hp worms *in vitro*. Splenic Treg isolated from mice at 5 days after Py infection were cultured with Hp products (100 μg/mL) or living Hp worms using a transwell system in the presence of DCs. Cultured Treg were used for suppressive analyses as described in the legend for Fig. 3C. Data are presented as the means ± SE of triplicate samples in a representative of 3–5 repeated experiments. There are no significant differences among the Treg conditioning treatments by Student's t-test.

responses in mice co-infected with Hp may prohibit the development of protective Th1 responses such as the production of IFN-γ.

Infections with helminths have also been reported to activate Treg [25, 28], and Hp suppresses allergic responses to innoxious Ag or protective immunity against pathogens in a Treg-dependent manner [29]. Su *et al.* [18] described the induction of regulatory cytokines, such as TGF-β and IL-10, during co-infection with Hp and *P. chabaudi*. We observed as well that transcription of TGF-β and IL-10 of Treg isolated from co-infected mice was slightly increased compared with those from non-infected animals or infected with either Py or Hp (data not shown). It would be interesting to evaluate the importance of these regulatory cytokines in *in vitro* suppressive function analysis, as done in Fig. 3C for instance.

The ES Ag of Hp were reported to be immunosuppressive toward T cells [30, 31]. However, we observed that infection with Hp alone did not activate Treg *in vivo* and that neither Hp products nor living worms directly activated Treg *in vitro*. Previous report suggested that Hp activates Treg *via* DC [32], but our *in vitro* results showed that Hp did not induce significant activation of Treg even in the co-culture with DC, suggesting less probability of the pathway between Hp *ex vivo* and strongly activated Treg, either dependently or independently of DC. One possibility may be that Hp infection takes longer than 2 wk to activate Treg by itself. Su *et al.* [18] described that mortality of co-infected mice increased if *P. chabaudi* infection was performed later than 2 wk after Hp infection. However, when we compared the effect of interval from preceding Hp to following Py infection on the induction of Treg between 2 and 6 wk (data not shown), Treg from both sets of co-infected mice showed similar and significant suppression compared with those from Py-infected mice, while Treg from Hp-infected mice did not show significant suppression. Taken together, our results suggest that Hp infection does not directly induce Treg activation, but probably conditions the host to stand by for Treg activation on exposure to incoming Ag /pathogens and/or enhances Treg activation by other stimulations such as Py.

Finally, our results demonstrate that co-infection with intestinal nematodes deteriorates the course of malaria, which is supposed to reflect the infectious state in malaria-endemic areas. Although we did not address whether treatment with anti-helminthic drugs improves malaria, chemotherapy against helminths would be included in global malaria control.

Materials and methods

Mice and parasites

Male 8- to 10-wk-old C57BL/6 mice were purchased from Kyudo (Tosu, Japan). All experiments using mice were conducted according to the guidelines for animal experimentation of Kyushu University.

Hp was kindly provided by Dr. J. F. Urban, Jr. (Beltsville Human Nutrition Research Center, US Department of Agriculture, Beltsville, MD, USA) and maintained by *in vivo* passages using male ICR mice. For infection, feces containing eggs were incubated on wet filter paper to allow the eggs to develop into infective larvae. Mice were infected orally with 200 infective larvae by gastric intubation. Infection was confirmed by Hp egg detection in feces before and after Py infection.

pRBC (2.5×10^4 cells/mouse) were commonly injected i.p., and the percent parasitemia (ratio of pRBC to total RBCs) was monitored by microscopic evaluation of thin blood films stained with Giemsa solution. For depletion of $CD25^+$ T cells *in vivo*, mice were injected i.p. with 100 μg of anti-CD25 Ab 1 day before and 1 day after Py infection. Each infection experiment was repeated three times with 5–7 mice *per* group.

Reagents

PE-anti-CD25 (PC61.5), allophycocyanin-anti-CD4 (GK1.5) and FITC-anti-Foxp3 (FJK-16s) staining kits, as well as FITC-anti-CD11c

(N418) Ab were obtained from eBioscience (San Diego, CA, USA). Anti-PE, anti-allophycocyanin and anti-FITC microbeads (Miltenyi Biotec, GmBH, Bergisch Gladbach, Germany) were used for cell purification. Monoclonal rat anti-mouse CD25 (7D4) IgM purified from the ascites of hybridoma-injected athymic nude mice was used for *in vivo* treatments.

Preparation of parasites and their products

Worm products were prepared as described previously [30, 31] with modifications. Adult Hp worms were collected from the upper gastrointestinal tract of infected mice at 3–4 wk after larvae infection. The worms were washed three times with PBS containing ampicillin (150 μg/mL; Sigma, St. Louis, MO, USA) and streptomycin (50 μg/mL; Sigma), and approximately 500–1000 worms were incubated in 0.5 mL of ampicillin/streptomycin/PBS for 24–48 h at 37°C. The culture supernatant was collected by centrifugation at 10 000 × *g* for 10 min at 4°C and used as the Hp ES Ag. Worms were mechanically homogenized after or before incubation, and frozen and thawed 3–5 times. The supernatant was collected by centrifugation at 10 000 × *g* for 10 min at 4°C and used as the Hp extract. As a negative control, non-Hp-infected mouse intestinal contents were prepared in the same manner as for Hp ES Ag. All products were filtered through 0.45-μm pore filters, quantified by the BCA™ Protein Assay (Pierce, Rockford, IL, USA) and stored at –80°C until use. The products were pretreated with polymyxin B (50 μg/mL; Sigma) for 30 min before dilution with cell culture medium to a final concentration of 100 μg/mL, including 12.5 μg/mL polymyxin B. When required, living worms were freshly prepared by washing three times with PBS containing ampicillin and streptomycin and pretreated with polymyxin B for 30 min at room temperature. Hp products were prepared for each cellular experiment.

pRBC were isolated using a Percoll enrichment technique [33]. Briefly, blood from Py-infected mice was collected into heparinized PBS and passed through a cellulose column to remove leukocytes and platelets. After addition of the RBC solution to 63% v/v Percoll/PBS and centrifugation, pRBC were collected from the interphase. pRBC were freshly prepared for each cellular experiment. When required, isolated pRBC were frozen and thawed three times, and the supernatant was collected by centrifugation at 10 000 × *g* for 10 min at 4°C for use as a coating Ag in ELISA.

Cell purification

Cell purification was performed using a magnetic cell sorting system (Miltenyi Biotech GmBH) according to the manufacturer's instructions. Spleens of mice were reduced to single cell suspensions by hemolysis with 0.86% NH_4Cl. To purify $CD4^+$ $CD25^-$ cells, the suspensions were incubated with FITC-anti-CD4 and PE-anti-CD25 Ab, followed by the addition of anti-PE microbeads and removal of $CD25^+$ cells. Anti-FITC microbeads were added to the flowthrough and $CD4^+CD25^-$ cells were obtained. DCs were purified using an FITC-anti-CD11c Ab. Treg were purified using a PE-anti-CD25 Ab, and 90% of them were confirmed to express CD4, CD25 and Foxp3 by flow cytometry. The purity of each cell subset usually exceeded 90%.

Cell culture

Purified T cells were cultured with pRBC in the presence of $CD11c^+$ cells in 200 μL of RPMI1640 supplemented with 100 IU/mL penicillin, 100 μg/mL streptomycin, 20 mM HEPES, 50 mM $NaHCO_3$, 2 mM L-glutamine, 100 μM 2-mercaptoethanol and 10% inactivated fetal bovine serum on round-bottomed 96-well plates. ConA was added as an assay control at a final concentration of 2.5 μg/mL. $CD11c^+$ cells were irradiated with 30 Gy before coculture with other cells. Typically, 1×10^5 T cells, $1–2 \times 10^5$ pRBC and 1×10^4 $CD11c^+$ cells were cocultured *per* well. Cultures were performed for 68–76 h at 37°C in air supplemented with 5% CO_2, including 10–16 h of coculture with ^{3}H-thymidine (1 μCi/well). Cells were harvested onto glass–fiber filter mats, dried and measured for their ^{3}H-thymidine uptake using a liquid scintillation counter. When required, the supernatant was collected before the addition of ^{3}H-thymidine and kept at –80°C until use. Each triplicate experiment was repeated 3–6 times.

Treg suppression assay

To analyze Treg functions, purified $CD4^+CD25^-$ cells (1×10^5 cells/well) from uninfected or infected mouse spleens stimulated with soluble ConA (2.5 μg/mL) and $CD11c^+$ cells (1×10^4 cells/well) from uninfected mouse spleens were cultured with a variety of freshly isolated or preconditioned Treg at various populations for 72 h and incubated with ^{3}H-thymidine (1 μCi/well) for the last 8–12 h. Radioactivity was measured using a liquid scintillation counter.

When required, purified Treg isolated from uninfected or Py-infected mouse spleens were preconditioned with $CD11c^+$ cells from uninfected mouse spleens under various conditions for 72 h. Conditioning with living Hp worms was performed using a transwell system (0.2-μm Anopore membrane; Nalge Nunc International, Rochester, NY, USA), in which the cells were in the lower chamber and 10 worms were in the upper chamber. Conditioned Treg were washed once, counted for living cells by Trypan blue staining and used for suppression assays as described above. Each triplicate experiment was repeated 3–5 times.

ELISA

The IFN-γ concentrations in the above-described cell culture supernatants were measured using a Mouse IFN-γ ELISA

Development Kit, DuoSet (R&D Systems, Minneapolis, MN, USA) according to the manufacturer's instructions. Each duplicate experiment was repeated three times. The anti-malaria Ab titers in the sera of mice were measured by ELISA by the OD at 440 nm using HRP-anti-mouse IgG(H+L), HRP-anti-mouse IgG1 and HRP-anti-mouse IgG2a Ab as previously described [34]. Sera were collected and kept at –80°C until analysis. Malaria Ag was prepared as described above and used as a coating Ag. Each triplicate experiment was repeated three times.

Flow cytometry

Splenocytes were prepared as single cell suspensions by hemolysis with 0.86% NH_4Cl. After staining of cell surface molecules or intracellular staining of Foxp3, the cells were evaluated using a FACSCalibur (BD, Franklin Lakes, NJ, USA) according to the manufacturer's instructions and the data were analyzed with the CellQuest Pro software (BD). Each infection experiment using 2–3 mice was repeated three times.

Statistical analysis

Student's *t*-test was used for statistical analyses. Values of $p<0.05$ were considered significant.

Acknowledgements: This study was supported by the Ministry of Education, Science, Sport and Culture of Japan (Grant 1890400, 19041056). The authors appreciate the special kindness of Dr. J. F. Urban Jr., Beltsville Human Nutrition Research Center, US Department of Agriculture, Beltsville, MD, USA, who provided the larvae of *Heligmosomoides polygyrus* used in this study.

Conflict of interest: The authors declare no financial or commercial conflict of interest.

References

1 **Barry, A. E., Leliwa-Sytek, A., Tavul, L., Imrie, H., Migot-Nabias, F., Brown, S. M., McVean, G. A. V. *et al.***, Population genomics of the immune evasion (*var*) genes of *Plasmodium falciparum*. *PLoS Pathogens* 2007. **3**: e34.

2 **Healer, J., Murphy, V., Hodder, A. N., Masciantonio, R., Gemmill, A. W., Anders, R. F., Cowman, A. F. *et al.***, Allelic polymorphisms in apical membrane antigen-1 are responsible for evasion of antibody-mediated inhibition in *Plasmodium falciparum*. *Mol. Microbiol.* 2004. **52**: 159–168.

3 **Walther, M., Tongren, J. E., Andrews, L., Korbel, D., King, E., Fletcher, H., Andersen, R. F. *et al.***, Upregulation of TGF-beta, FOXP3, and $CD4^+CD25^+$ regulatory T cells correlates with more rapid parasite growth in human malaria infection. *Immunity* 2005. **23**: 287–296.

4 **Hisaeda, H., Maekawa, Y., Iwakawa, D., Okada, H., Himeno, K., Kishihara, K., Tsukumo, S. and Yasutomo, K.**, Escape of malaria parasites from host immunity requires $CD4^+CD25^+$ regulatory T cells. *Nat. Med.* 2004. **10**: 29–30.

5 **Xu, H., Wipasa, J., Yan, H., Zeng, M., Makobongo, M. O., Finkelman, F. D., Kelso, A. and Good, M. F.**, The mechanism and significance of deletion of parasite-specific $CD4^+$ T cells in malaria infection. *J. Exp. Med.* 2002. **195**: 881–892.

6 **Urban, B. C., Ferguson, D. J. P., Pain, A., Willcox, N., Plebansk, M., Austyn, J. M. and Roberts, D. J.**, *Plasmodium falciparum*-infected erythrocytes modulate the maturation of dendritic cells. *Nature* 1999. **400**: 73–77.

7 **March, K. and Snow, R. W.**, Malaria transmission and morbidity. *Parasitologia* 1999. **41**: 241–246.

8 **Shankar, A. H.**, Nutritional modulation of malaria morbidity and mortality. *J. Infect. Dis.* 2000. **182**: S37–S53.

9 **Barnes, K. I., Durrheim, D. N., Little, F., Jackson, A., Mehta, U., Allen, E., Dlamini, S. S. *et al.***, Effect of artemether-lumefantrine policy and improved vector control on malaria burden in KwaZulu-Natal, South Africa. *PLoS Med.* 2005. **2**: e330.

10 **Abu-Raddad, L. J., Patnaik, P. and Kublin, J. G.**, Dual infection with HIV and malaria fuels the spread of both diseases in sub-Saharan Africa. *Science* 2006. **312**: 1603–1606.

11 **World Health Organization**, 2004. Malaria cases (per 100,000) by country, latest available data. Accessed on 28th January 2009.

12 **World Health Organization**, 2006. Soil-transmitted helminth (STH) infections are widely distributed in tropical and subtropical areas – 2006. Accessed on 28th January 2009.

13 **Jenkins, S. J., Hewitson, J. P., Jenkins, G. R. and Mountford, A. P.**, Modulation of the host's immune response by schistosome larvae. *Parasite Immunol.* 2005. **27**: 385–393.

14 **Hoerauf, A., Satoguina, J., Saeftel, M. and Specht, S.**, Immunomodulation by filarial nematodes. *Parasite Immunol.* 2005. **27**: 417–429.

15 **Maizels, R. M. and Yazdanbakhsh, M.**, Immune regulation by helminth parasites: cellular and molecular mechanisms. *Nat. Rev. Immunol.* 2003. **3**: 733–744.

16 **Nacher, M., Singhasivanon, P., Yimsamran, S., Manibunyong, W., Thanyavanich, N., Wuthisen, P. and Looareesuwan, S.**, Intestinal helminth infections are associated with increased incidence of *Plasmodium falciparum* malaria in Thailand. *J. Parasitol.* 2002. **88**: 55–58.

17 **Nacher, M., Gay, F., Singhasivanon, P., Krudsood, S., Treeprasertsuk, S., Mazier, D., Vouldoukis I. and Looareesuwan, S.**, *Ascaris lumbricoides* infection is associated with protection from cerebral malaria. *Parasite Immunol.* 2000. **22**: 107–113.

18 **Su, Z., Segura, M., Morgan, K., Loredo-Osti, J. C. and Stevenson, M. M.**, Impairment of protective immunity to blood-stage malaria by concurrent nematode infection. *Infect. Immun.* 2005. **73**: 3531–3539.

19 **Noland, G. S., Urban, J. F., Jr. , Fried, B. and Kumar, N.**, Counter-regulatory anti-parasite cytokine responses during concurrent *Plasmodium yoelii* and intestinal helminth infections in mice. *Exp. Parasitol.* 2008. **119**: 272–278.

20 **Tetsutani, K., Ishiwata, K., Torii, M., Hamano, S., Hisaeda, H. and Himeno, K.**, Concurrent infection with *Heligmosomoides polygyrus* modulates murine host response against *Plasmodium berghei* ANKA infection. *Am. J. Trop. Med. Hyg.* 2008. **79**: 819–822.

21 **Gause, W. C., Urban, J. F., Jr., and Stadecker, M. J.**, The immune response to parasitic helminths: insights from murine models. *Trends Immunol.* 2003. **24**: 269–277.

22 **Monroy, F. G. and Enriquez, F. J.**, *Heligmosomoides polygyrus*: a model for chronic gastrointestinal helminthiasis. *Parasitol. Today* 1992. **8**: 49–54.

23 Adachi, K., Tsutsui, H., Kashiwamura, S., Seki, E., Nakano, H., Takeuchi, O., Takeda, K. et al., *Plasmodium berghei* infection in mice induces liver injury by an IL-12-and toll-like receptor/myeloid differentiation factor 88-dependent mechanism. *J. Immunol.* 2001. **167**: 5928–5934.

24 Shear, H. L., Srinivasan, R., Nolan, T. and Ng, C., Role of IFN-γ and nonlethal malaria in susceptible and resistant murine hosts. *J. Immunol.* 1989. **143**: 2038–2044.

25 Finney, C. A. M., Taylor, M. D., Wilson, M. S. and Maizels, R. M., Expansion and activation of $CD4^+CD25^+$ regulatory T cells in *Heligmosomoides polygyrus* infection. *Eur. J. Immunol.* 2007. **37**: 1874–1886.

26 Ohata, J., Miura, T., Johnson, T. A., Hori, S., Ziegler, S. F. and Kohsaka, H., Enhanced efficacy of regulatory T cell transfer against increasing resistance, by elevated Foxp3 expression induced in arthritic murine hosts. *Arthritis Rheum.* 2007. **56**: 2947–2956.

27 Couper, K. N., Blount, D. G., de Souza, J. B., Suffia, I., Belkaid, Y. and Riley, E. M., Incomplete depletion and rapid regeneration of $Foxp3^+$ regulatory T cells following anti-CD25 treatment in malaria-infected mice. *J. Immunol.* 2007. **178**: 4136–4146.

28 Watanabe, K., Mwinzi, P. N., Black, C. L., Muok, E. M., Karanja, D. M., Secor, W. E. and Colley, D. G., T regulatory cell levels decrease in people infected with *Schistosoma mansoni* on effective treatment. *Am. J. Trop. Med. Hyg.* 2007. **77**: 676–682.

29 Wilson, M. S., Taylor, M. D., Balic, A., Finney, C. A. M, Lamb, J. R. and Maizels, R. M., Suppression of allergic airway inflammation by helminth-induced regulatory T cells. *J. Exp. Med.* 2005. **202**: 1199–1212.

30 Telford, G., Wheeler, D. J., Appleby, P., Bowen, J. G. and Pritchard, D. I., *Heligmosomoides polygyrus* immunomodulatory factor (IMF), targets T-lymphocytes. *Parasite Immunol.* 1998. **20**: 601–611.

31 Rzepecka, J., Lucius, R., Doligalska, M., Beck, S., Rausch, S. and Hartmann, S., Screening for immunomodulatory proteins of the intestinal parasitic nematode *Heligmosomoides polygyrus*. *Parasite Immunol.* 2006. **28**: 463–472.

32 Segura, M., Su, Z., Piccirillo, C. and Stevenson, M. M., Impairment of dendritic cell function by excretory-secretory products: a potential mechanism for nematode-induced immunosuppression. *Eur. J. Immunol.* 2007. **37**: 1887-1904.

33 Tosta, C. E., Sedegah, M., Henderson, D. C. and Wedderburn, N., *Plasmodium yoelii* and *Plasmodium berghei*: isolation of infected erythrocytes from blood by colloidal silica gradient centrifugation. *Exp. Parasitol.* 1980. **50**: 7–15.

34 Matsuoka, Y., Malaria ELISA. In Tanabe, K., Waki, S., Kojima, S. and Kita, K. (Eds.), *Malariology Laboratory Manuals*. Kinokuniya, Tokyo 2000, pp. 123–126.

Abbreviations: **ES:** excretory/secretory · **Foxp3:** forkhead box p3 · **Hp:** *Heligmosomoides polygyrus* · **pRBC:** *Plasmodium yoelii*-parasitized erythrocyte · **Py:** *Plasmodium yoelii* 17XNL

Full correspondence: Dr. Kohhei Tetsutani, Department of Parasitology, Kyushu University Graduate School of Medical Science, 3-1-1 Maidashi, Higashi-ku, Fukuoka 812-0054, Japan
Fax: +81-92-642-6118
e-mail: tetztani@gmail.com

Received: 18/3/2009
Revised: 8/5/2009
Accepted: 24/6/2009

Parasitology International 58 (2009) 29–35

Contents lists available at ScienceDirect

Parasitology International

journal homepage: www.elsevier.com/locate/parint

Rhoptry neck protein RON2 forms a complex with microneme protein AMA1 in *Plasmodium falciparum* merozoites☆

Jun Cao [a,b], Osamu Kaneko [a,c,*], Amporn Thongkukiatkul [d], Mayumi Tachibana [a], Hitoshi Otsuki [a], Qi Gao [b], Takafumi Tsuboi [e,f], Motomi Torii [a]

[a] Department of Molecular Parasitology, Ehime University Graduate School of Medicine, Shitsukawa, Toon, Ehime 791-0295, Japan
[b] Malaria Department, Jiangsu Institute of Parasitic Diseases, Meiyuan, Wuxi, Jiangsu 214064, People's Republic of China
[c] Department of Protozoology, Institute of Tropical Medicine (NEKKEN), Nagasaki University, Sakamoto, Nagasaki 852-8523, Japan
[d] Department of Biology, Faculty of Science, Burapha University, Chonburi 20131, Thailand
[e] Cell-Free Science and Technology Research Center, Ehime University, Matsuyama, Ehime 790-8577, Japan
[f] Venture Business Laboratory, Ehime University, Matsuyama, Ehime 790-8577, Japan

ARTICLE INFO

Article history:
Received 12 August 2008
Received in revised form 15 September 2008
Accepted 18 September 2008
Available online 7 October 2008

Keywords:
AMA1
Erythrocyte invasion
Merozoite
Plasmodium falciparum
Rhoptry

ABSTRACT

Erythrocyte invasion is an essential step in the establishment of host infection by malaria parasites, and is a major target of intervention strategies that attempt to control the disease. Recent proteome analysis of the closely-related apicomplexan parasite, *Toxoplasma gondii*, revealed a panel of novel proteins (RONs) located at the neck portion of the rhoptries. Three of these proteins, RON2, RON4, and RON5 have been shown to form a complex with the microneme protein Apical Membrane Protein 1 (AMA1). This complex, termed the Moving Junction complex, localizes at the interface of the parasite and the host cell during the invasion process. Here we characterized a RON2 ortholog in *Plasmodium falciparum*. *Pf*RON2 transcription peaked at the mature schizont stage and was expressed at the neck portion of the rhoptry in the merozoite. Co-immunoprecipitation of *Pf*RON2, *Pf*RON4 and *Pf*AMA1 indicated that the complex formation is conserved between *T. gondii* and *P. falciparum*, suggesting that co-operative function of the rhoptry and microneme proteins is a common mechanism in apicomplexan parasites during host cell invasion. *Pf*RON2 possesses a region displaying homology with the rhoptry body protein *Pf*RhopH1/Clag, a component of the RhopH complex. However, here we present co-immunoprecipitation studies which suggest that *Pf*RON2 is not a component of the RhopH complex and has an independent role. Nucleotide polymorphism analysis suggested that *Pf*RON2 was under diversifying selective pressure. This evidence suggests that RON2 appears to have a fundamental role in host cell invasion by apicomplexan parasites, and is a potential target for malaria intervention strategies.

1. Introduction

Malaria is one of the most prevalent and deadly global infectious diseases, more than half of the world's population is at the risk of infection, and over 300 million people develop clinical disease each year of which 2 million are fatal [1]. Clinical malaria results from the replication of protozoan parasites of the genus *Plasmodium* in the circulating erythrocytes of the host. During the time between release from a rupturing mature schizont-infected erythrocyte and invasion of new erythrocytes, merozoites are transiently exposed in the circulation, and are thus potentially vulnerable to attack by preventive measures based upon immunological or biochemical methods. To design such tools, it is important to understand the molecular composition of the merozoite and the structure-function makeup of the molecular interactions that occur as the merozoite recognizes and gains entry into a host cell.

Like most apicomplexan parasites, the malaria merozoite invades host cells via a multistep process initiated by reversible binding to the erythrocyte surface. Subsequently, a high affinity attachment occurs between the apical end of the merozoite and the host cell, followed by the movement of the junctional adhesion zone (moving junction) around the merozoite toward its posterior pole. Finally the merozoite invaginates into the erythrocyte by forming a nascent parasitophorous vacuole [2]. The moving junction is one of the most distinctive features of apicomplexan invasion and was first observed in

Abbreviations: aa, amino acid(s); Ab, antibody; AMA1, apical membrane antigen 1; GST, Glutathione S transferase; PBS, phosphate-buffered saline; PCR, polymerase chain reaction; RON, rhoptry neck protein.

☆ Sequence data from this article have been deposited with the GenBank™/EMBL/DDBJ databases under accession numbers AB444588–AB444592.

* Corresponding author. Department of Protozoology, Institute of Tropical Medicine (NEKKEN), Nagasaki University, Sakamoto, Nagasaki 852-8523, Japan. Tel.: +81 95 819 7838; fax: +81 95 819 7805.
E-mail address: okaneko@nagasaki-u.ac.jp (O. Kaneko).

1383-5769/$ – see front matter © 2008 Elsevier Ireland Ltd. All rights reserved.
doi:10.1016/j.parint.2008.09.005

Plasmodium species in the late 1970s [3], but the molecular nature of its structure remains unresolved.

Recent studies in *Toxoplasma gondii* suggest that host cell invasion involves protein discharge from at least two apical secretory organelles, the micronemes and rhoptries, based on the observation that a microneme protein, Apical Membrane Protein 1 (AMA1), forms a complex with three rhoptry neck (RON) proteins: RON2, RON4 and Ts4705 (RON5) [4–6]. These proteins have predicted orthologs in *P. falciparum*, and the RON4 ortholog has been reported to associate with *Pf*AMA1 [7] and to be localized at the moving junction [8], suggesting that the complex (and likely its function) is conserved between *T. gondii* and *P. falciparum* [7]. Attempts to knock-out the AMA1 gene locus were unsuccessful in both *Plasmodium* [9] and *T. gondii* [10], and the conditional reduction of *Tg*AMA1 expression severely impaired the cell invasion ability of *T. gondii* [11], indicating AMA1 has an essential function. The conservation of the RON proteins among apicomplexan parasites suggest that their functions and protein interactions are also conserved in the biology of host cell invasion. However, in *Plasmodium*, the details of this complex have yet to be fully characterized. In this study, to better understand the moving junction complex formation in *Plasmodium*, we sought to characterize *Pf*RON2 and determine the nature of its interaction with *Pf*RON4 and *Pf*AMA1.

2. Materials and methods

2.1. Malaria parasites

P. falciparum cloned lines 3D7, HB3, Dd2, 7G8, FVO, and D10 were maintained *in vitro*, essentially as previously described [12].

2.2. DNA and RNA isolation

Genomic DNA (gDNA) was isolated from *P. falciparum* using IsoQuick™ (Orca Research Inc., Bothell, WA). To determine transcription levels throughout the asexual stages, schizonts were purified by differential centrifugation on a 70%/40% Percoll-sorbitol gradient, after which released merozoites were allowed to invade uninfected erythrocytes for 4 h before the clearance of all remaining schizonts using 5% D-sorbitol. Fractions of the culture were harvested immediately and 24 h later, and then at 6 h intervals thereafter. Total RNA was isolated from parasite-infected erythrocytes stored at −20 °C in RNA*later*™ (Qiagen, Valencia, CA), using the RNeasy Mini Kit (Qiagen). Following DNase treatment, complementary DNA (cDNA) was generated with random hexamers using an Omniscript Reverse Transcription Kit (Qiagen).

2.3. Polymerase chain reaction (PCR) amplification and sequencing

A TBLASTN search was performed against the *P. falciparum* genome database (3D7 parasite line) via PlasmoDB website (http://www.plasmodb.org/) [13] using the *Tg*RON2 amino acid sequence as a query. To evaluate the polymorphism of *Pf*RON2, five pairs of overlapping primers were used for PCR amplification from HB3, FVO, Dd2, D10, and 7G8 parasite lines, and sequences were determined by direct sequencing of the PCR-amplified DNA fragments using an ABI PRISM® 3100-*Avant* Genetic Analyzer (Applied Biosystems, Foster City, CA). Oligonucleotides used were as follows: fRON2.F2 (5′-GATTCCAATAATTATAATTCTGATAATG-3′) and fRON2.R2 (5′-CGTAAAATATTCATTATATGAAAGATATGC-3′), fRON2.F3 (5′-GCATTAGGAGAACTTGTTGAACCA-3′) and fRON2.R3 (5′-CATAATATCTAAATAGGTTTTTGCTGAC-3′), fRON2.F4 (5′-GGATTAGTATTTTTATATGCAATGATTG-3′) and fRON2.R4 (5′-GTTATTTTCTAATAAATGTTTACTATCTTC-3′), fRON2.F5 (5′-GATAAATGGGATCAATTTATAAATAAGG-3′) and fRON2.R5 (5′-GCTAGCTACTGGTCCTGCACCT-3′), and fRON2.F6 (5′-ATGCAATTACCTTACTTAAGTCAAATG-3′) and fRON2.R6 (5′-ATATAAAATGAAAATAACAGAAAAGGTTATG-3′).

2.4. Quantification of pfron2 transcripts

Transcription of *ron2* was evaluated in the HB3 parasite line by real-time reverse transcription (RT)-PCR using a QuantiTect SYBR Green PCR Kit (Qiagen) and a LightCycler System (Roche, Basel, Switzerland). As a control, transcription of *ama1* and *rhoph2* was also evaluated. Oligonucleotides used were as follows: fRON2.qF (5′-CAGAACTAAGCAAACATGTAAAACATG-3′) and fRON2.qR (5′-GTATAACGCCTTGCTCATTTCCTG-3′) for *pfron2* (product size is 133 bp); fAMA1.qF (5′-GGAAGAGGACAGAATTATTGGGAAC-3′) and fAMA1.qR (5′-CCTGAATCTTCTTGTTGGTATGTATG-3′) for *pfama1* (product size is 137 bp); fRhopH2.qF (5′-GTAACAACACTTACTAAGGCAGACT-3′) and fRhopH2.qR (5′-GTACAAAGCTACAATATTGTTAGATCT-3′) for *pfrhoph2* (product size is 210 bp). The same oligonucleotides were used to PCR-amplify DNA fragments to be ligated into the pGEM-T Easy® plasmid (Promega, Madison, WI) which was used to make a standard curve to evaluate the copy number of each transcript.

2.5. Antibodies

A DNA fragment encoding amino acid positions (aa) 21–98 of *Pf*RON2 was PCR-amplified from *P. falciparum* 3D7 gDNA and ligated into pEU-E01GST-N2, an expression plasmid with N-terminal glutathione S transferase (GST)-tag followed by a PreScission Protease cleavage site, designed specifically for the wheat germ cell-free protein expression system (CellFree Sciences Co., Ltd., Matsuyama, Japan) [14], to produce recombinant GST-fused fRON2N protein (GST-fRON2N). Oligonucleotides used in the PCR amplification were fRON2.SalF1 (5′-*GTCGAC*TCAGAACTAAGCAAACATGTAAAACATG-3′) and fRON2.SalR1 (5′-*GTCGAC*CCCATTATTCATTTCACTACCAGGA-3′) (SalI restriction sites are underlined). Produced GST-fRON2N was captured using a glutathione-Sepharose 4B column and eluted with 10 mM reduced gluthathione, pH 8.0. To generate anti-*Pf*RON2 sera, BALB/c mice were immunized subcutaneously with 20 μg of purified GST-fRON2N emulsified with Freund's adjuvant. A Japanese white rabbit was immunized subcutaneously with 500 μg of purified GST-fRON2N with Freund's adjuvant for the first time, followed by 250 μg thereafter. All immunizations were done 4 times at 3 week intervals, prior to collection of antisera. Rabbit anti-*Pf*RhopH2 serum was obtained from I. Ling (National Institute for Medical Research, UK) [15], Rabbit anti-*Pf*AMA1 serum was obtained from C. Long (National Institute of Health, USA), and mouse monoclonal anti-*Pf*RON4 antibody (Ab; 26C64F12) was obtained from J.-F. Dubremetz (Université de Montpellier 2, France) [7]. Rabbit anti-Clag3.1 serum was as previously described [16].

2.6. SDS-PAGE and Western blot analysis

The recombinant protein, GST-fRON2N, was digested with a PreScission Protease at 4 °C overnight before analysis. Triton X-100 extracts of *P. falciparum* or recombinant proteins were dissolved in SDS-PAGE loading buffer, incubated at 100 °C for 3 min, and subjected to electrophoresis under reducing conditions on a 5–20% polyacrylamide gel (ATTO, Japan). Proteins were then transferred to a 0.22 μm PVDF membrane (BioRad, Hercules, CA). The proteins were immunostained with antisera followed by horseradish peroxidase-conjugated secondary Ab (Biosource Int., Camarillo, CA) and visualized with Immobilon™ Western Chemiluminescent HRP Substrate (Millipore, Billerica, MA) on RX-U film (Fuji, Japan). The relative molecular sizes of the parasite-encoded proteins were calculated by reference to molecular size standards (BioRad).

2.7. Immunoprecipitation

Immunoprecipitation was carried out as previously described [17]. Briefly, proteins were extracted from late schizont parasite pellets by

1% Triton X-100 treatment in phosphate-buffered saline (PBS) containing cOmplete Proteinase Inhibitor Cocktail Tablets (Roche). Supernatants (50 μl) were pre-incubated at 4 °C for 1 h with 20 μl of 50% protein G-conjugated beads (GammaBind Plus Sepharose; GE Healthcare) in NETT buffer (50 mM Tris–HCl, 0.15 M NaCl, 1 mM EDTA, and 0.5% Triton X-100) supplemented with 0.5% BSA (fraction V; Sigma-Aldrich). Recovered supernatants were incubated with rabbit antisera (anti-*Pf*RON2, anti-*Pf*AMA1, or anti-*Pf*RhopH2) or mouse anti-*Pf*RON4 Ab with gentle rotation at 4 °C for 2 h and then 20 μl of 50% protein G-conjugated beads were added. After 1 h incubation at 4 °C, the beads were washed once with NETT-0.5% BSA, once with NETT, once with high-salt NETT (0.5 M NaCl), once with NETT, and once with low-salt NETT (0.05 M NaCl and 0.17% Triton X-100). Finally, proteins were extracted from the protein G-conjugated beads by incubation with SDS-PAGE reducing loading buffer at 100 °C for 3 min. Supernatants were collected for Western blot analysis.

2.8. Indirect immunofluorescence assay

Thin smears of schizont-enriched *P. falciparum*-infected erythrocytes (Dd2 parasite line) were prepared on glass slides and stored at −80 °C. The smears were thawed, formaldehyde-fixed, and preincubated with PBS containing 5% non-fat milk at 37 °C for 30 min. They were then incubated with antisera at 37 °C for 1 h, followed by fluorescein isothiocyanate (FITC)-conjugated goat anti-(IgG and IgM) secondary Ab (Jackson ImmunoResearch Laboratories, West Grove, PA) and Alexa546-conjugated goat anti-(IgG and IgM) secondary Ab (Invitrogen, Carlsbad, CA) at 37 °C for 30 min. Nuclei were stained with 4′,6-diamidino-2-phenylindole (DAPI). Slides were mounted in ProLong Gold antifade reagent (Invitrogen) and viewed under oil-immersion. High resolution image-capture and processing were performed using a confocal scanning laser microscope (LSM5 PASCAL; Carl Zeiss MicroImaging, Thornwood, NY). Images were processed in Adobe Photoshop (Adobe Systems Inc., San José, CA).

2.9. Immunoelectron microscopy

Parasites were fixed for 15 min on ice in a mixture of 1% paraformaldehyde–0.1% glutaraldehyde in 0.1 M phosphate buffer (pH 7.4). Fixed specimens were washed, dehydrated, and embedded in LR White resin (Polysciences, Inc., Warrington, PA) as previously described [18,19]. Thin sections were blocked at 37 °C for 30 min in PBS containing 5% non-fat milk and 0.01% Tween 20 (PBS-MT). Grids were then incubated at 4 °C overnight with mouse anti-*Pf*RON2 or control sera in PBS-MT. After washing with PBS containing 10% BlockAce (Yukijirushi, Sapporo, Japan) and 0.01% Tween 20 (PBS-BT), the grids were incubated at 37 °C for 1 h with goat anti-mouse IgG conjugated to 10 nm gold particles (Amersham Life Science, Arlington, IL) diluted 1:20 in PBS-MT, rinsed with PBS-BT, and fixed on ice for 10 min in 2.5% glutaraldehyde to stabilize the gold. Then the grids were rinsed with distilled water, dried, and stained with uranyl acetate and lead citrate. Samples were examined with a transmission electron microscope (JEM-1230; JEOL Ltd., Tokyo, Japan).

2.10. Primary structure analysis of the protein

Signal peptide sequence was evaluated by SignalP3.0 [20]. Transmembrane region was evaluated by TMpred [21] and TMHMM2.0 [22]. Low complexity region was evaluated by Globplot 2.3 [23]. Amino acid sequence alignment was generated by MUSCLE [24].

2.11. Statistical analysis

Number of nonsynonymous substitutions over numbers of nonsynonymous sites (d_N), number of synonymous substitutions over numbers of synonymous sites (d_S), and their standard errors were computed using the Nei-Gojobori method with Jukes-Cantor correction implemented in MEGA 4.0.1 [25]. Standard errors were estimated using the bootstrap method with 500 replications. The statistical difference between d_N and d_S was tested using a one-tail *Z*-test with 500 bootstrap pseudosamples.

3. Results

3.1. RON2 orthologs of apicomplexan parasites

Using *Tg*RON2 as a query in BLAST analyses [26], and similar analyses using the predicted orthologs thus identified, we found RON2 orthologs in *P. falciparum* (*Pf*RON2; PF14_0495, PlasmoDB), *P. yoelii* 17XNL strain (*Py*RON2; PY06813, TIGR), *P. knowlesi* H strain (*Pk*RON2; PKH_125430 or PK14_2335w, Sanger Centre), and *P. vivax* Sal-I strain (*Pv*RON2; Pv117880, TIGR), *P. berghei* (*Pb*RON2; Contig5108), *P. chabaudi* (*Pch*RON2; Contig882.0), *Theileria annulata* (*Ta*RON2; Fig. S1A, TA19445 and TA19390, Sanger Centre [27]), *Theileria parva* (*Tp*RON2; Fig. S1B, TP01_0014, TIGR [28]), and *Babesia bigemina* (*Bbig*RON2; Fig. S1C, Contig3449, Sanger Centre). The RON2 were fragmented in the *P. berghei*, *P. chabaudi*, *T. annulata*, and *T. parva* genome nucleotide sequence databases, and full-length versions were constructed (supplementary Table S1).

3.2. PfRON2 protein structure and similarity to RhopH1/Clag proteins

The full-length *Pf*RON2 protein consists of 2189 residues with a putative signal peptide sequence at its N-terminus from amino acid positions (aa) 1 to 20. An interspecies variable region (aa 55–878), exhibiting low complexity and many repeats [23], was identified by comparing 6 *Plasmodium* RON2 amino acid sequences (Figs. 1 and S2). A BLASTP search using the conserved region of *Pf*RON2 (aa 879–2189) as a query identified *P. vivax* RhopH1/Clag homolog (XP_001616939.1, aa 251–394; E=0.001) as possessing homology with *Pf*RON2 aa 1105–1259. A Position-Specific Iterated BLAST search using *Pf*RON2 aa 1105–1259 as a query converged at iteration 3 and indentified most of the RhopH1/Clag genes in *Plasmodium* species. Alignment of RhopH1/Clag with RON2 from multiple genera identifies a predicted globular domain that is likely stabilized by disulfide bonds between 4 conserved Cys residues (Fig. 2). Three transmembrane regions were predicted by TMpred, however TMHMM2.0 predicted only a single transmembrane region for all *Plasmodium* RON2 orthologs assessed.. Interestingly, TMpred predicted a putative transmembrane region in the region conserved between RhopH1/Clag and RON2 (Fig. 2). Because RhopH1/Clag is a component of a soluble protein complex, we considered that these predicted transmembrane regions in RhopH1/Clag and RON2 constitute a likely hydrophobic region buried within a globular domain. Another predicted transmembrane region at aa 1114–1133 in *Pf*RON2 is also possibly hydrophobic region buried within a globular domain. TMpred considers the observation that there is an overrepresentation of positively charged amino acid

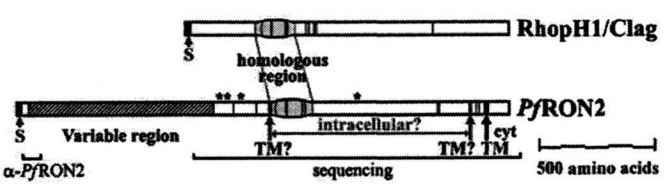

Fig. 1. Schematic representation of *Pf*RON2. S and TM indicate putative signal peptide (aa 1–20) and transmembrane sequences, respectively. The shaded box indicates an interspecies variable region. Vertical red bars indicate conserved Cys residues among orthologous sequences. Homologous region between RhopH1/Clag and RON2 is indicated by a yellow box. The region used to generate anti-*Pf*RON2 sera (α-*Pf*RON2) and the region sequenced in the laboratory lines (sequencing) are indicated. Asterisks indicate polymorphic sites.

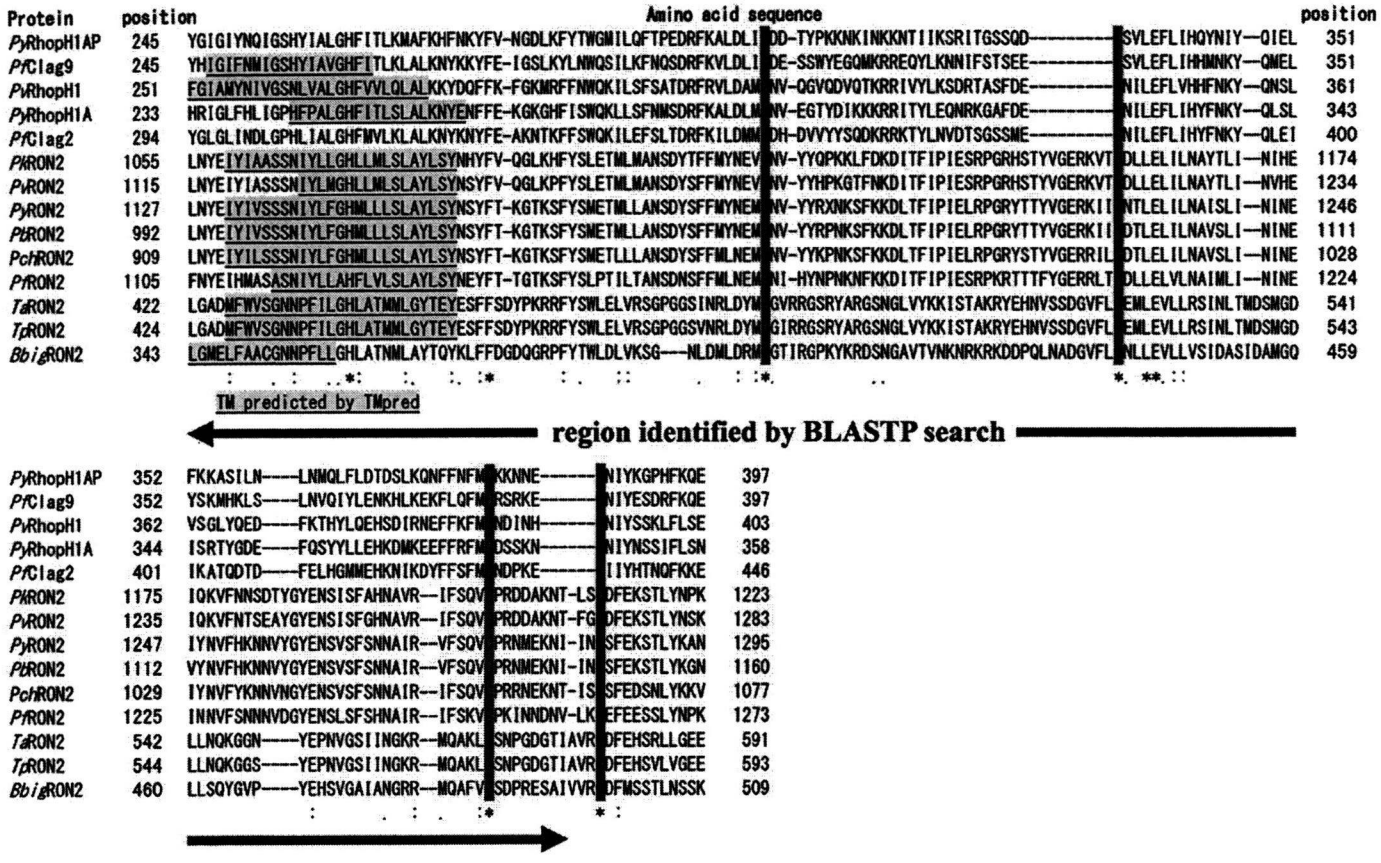

Fig. 2. Amino acid alignment of *Plasmodium* RON2 and RhopH1/Clag. Alignment was generated by MUSCLE [24] with manual correction. "*" indicates that the residues in that column are identical in all sequences in the alignment. ":" indicates conserved substitutions and "." indicates semi-conserved substitutions. In addition to 9 RON2 sequences, *P. falciparum* Clag2 (AAC71977), Clag9 (CAD52032), *P. yoelii* RhopH1A (BAB70675), RhopH1AP (BAB70677), and *Pv*RhopH1 (contig 1047) were used to generate the alignment. Cys residues are highlighted in red. The region possessing homology between RhopH1/Clag and RON2 as identified by BLASTP is indicated by the bar under the alignment.

residues in the cytoplasmic loops of the transmembrane protein [21], which is a likely explanation for this discrepancy.

3.3. *PfRON2 transcription peaks at the schizont stage*

To determine the transcription pattern in the asexual stages of the parasite life-cycle, quantitative RT-PCR was performed on the HB3 parasite line prepared from a synchronized culture harvested at 6 h intervals. Both RON2 and AMA1 transcriptions were seen to peak around 36–40 h after invasion, when parasites were in the schizont stage. AMA1 showed a broader and flatter transcription peak than RON2 (Fig. 3). Transcriptome data compiled in the PlasmoDB website [13,29] also indicated a milder wave crest of AMA1 transcripts compared with RON2.

3.4. *Complex formation of PfRON2, PfRON4, and PfAMA1*

Mouse and rabbit anti-*Pf*RON2 sera were generated using recombinant GST-fRON2N. Firstly, we evaluated the reactivity of anti-*Pf*RON2 sera by Western blot using recombinant proteins. Both antisera recognized the fRON2N component of the recombinant protein after cleavage (Fig. S3, filled arrows). Cleaved 26.4-kDa GST component (Fig. S3, arrowheads) and 46-kDa GST-fused PreScission protease (Fig. S3, unfilled arrow) were also recognized by these Abs.

Secondly, we evaluated the reactivity of these sera against native RON2 proteins extracted from schizont stage *P. falciparum* (HB3 line) by Western blot analysis. Both antisera reacted with a band slightly larger than 250 kDa (Fig. 4A, arrows), which is similar to the predicted molecular weight of *Pf*RON2 after exclusion of the putative signal peptide sequence (247 kDa). An 80-kDa band was detected by both mouse and rabbit antisera in HB3 extract, for which the exact identity is not known, but a possible processed product of *Pf*RON2. A 55-kDa band detected with rabbit antiserum was also detected with preimmune serum, suggesting that this band was unrelated to

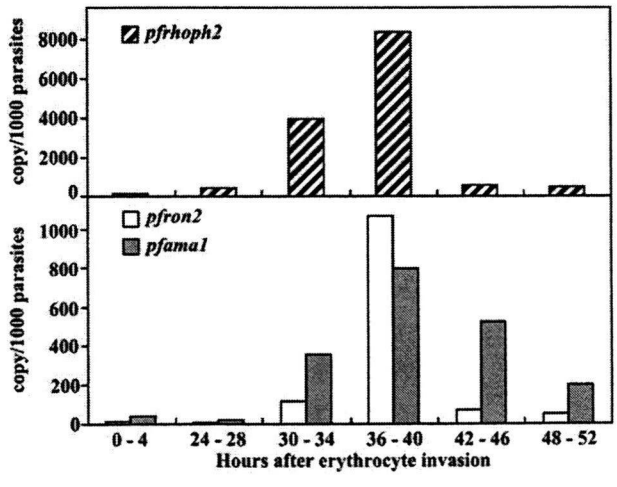

Fig. 3. Transcriptional analysis by quantitative RT-PCR of *pfrhoph2*, *pfron2*, and *pfama1* genes during blood stages of *P. falciparum* (HB3 line). *Y*-axis indicates copy number of each transcript detected per 1000 parasites. Similar results were observed in 3 independent experiments (data not shown).

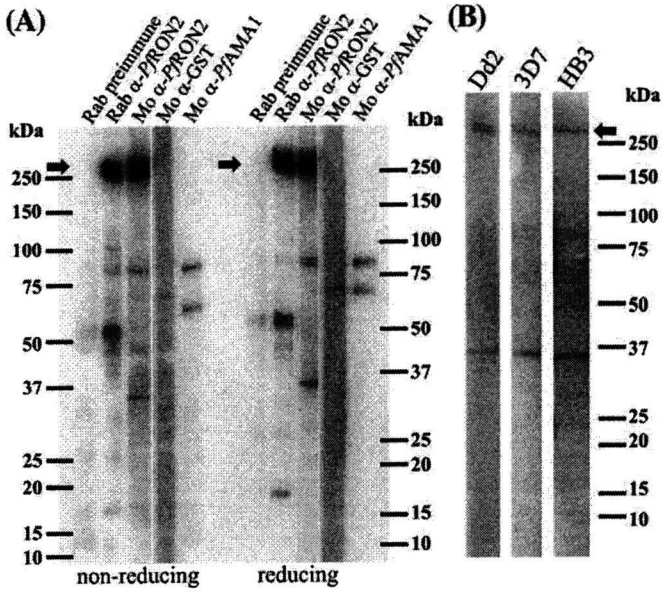

Fig. 4. Western blot analysis of antisera against native parasite proteins. (A) Schizont-enriched parasite extracts were stained by rabbit preimmune serum, (Rab preimmune), rabbit anti-*Pf*RON2 (Rab α-*Pf*RON2), mouse anti-fRON2N (Mo α-*Pf*RON2), and Abs against GST (Mo α-GST) or *Pf*AMA1 (Mo α-*Pf*AMA1) under both reducing and non-reducing conditions. Both mouse and rabbit anti-*Pf*RON2 sera detected a band slightly larger than 250 kDa. (B) Western blot of schizont-enriched parasite extracts from 3 different *P. falciparum* lines, Dd2, 3D7, and HB3 with mouse anti-fRON2N serum. Arrows indicate predicted *Pf*RON2 bands.

*Pf*RON2. A 35-kDa band was detected with mouse antiserum but not with rabbit antiserum, suggesting that it is also unrelated to RON2.

To evaluate the interaction between *Pf*RON2, *Pf*RON4, and *Pf*AMA1, we performed immunoblotting against immunoprecipitated materials from mature schizont-rich parasite extracts (Fig. 5). We found that RON2 was detected in the precipitated fraction using anti-*Pf*AMA1 or anti-*Pf*RON4. In the reciprocal experiment, *Pf*AMA1 and *Pf*RON4 were also detected in the precipitated fraction of anti-*Pf*RON2 serum. Although it is theoretically possible that such immunoprecipitated fractions contained the *Pf*RON2-*Pf*RON4, *Pf*RON2-*Pf*AMA1, and *Pf*RON4-*Pf*AMA1 dimeric complexes as appropriate to the primary

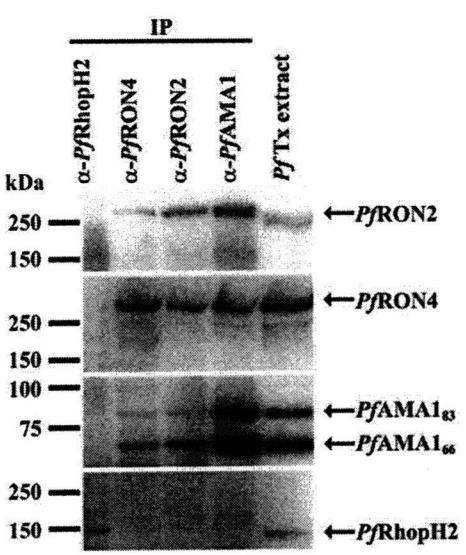

Fig. 5. *Pf*RON2 is co-precipitated with *Pf*RON4 and *Pf*AMA1. Schizont-rich parasite Triton X-100 extracts (*Pf* Tx extract) were immunoprecipitated (IP) with rabbit sera against *Pf*RhopH2 (α-*Pf*RhopH2), *Pf*RON2 (α-*Pf*RON2), *Pf*AMA1 (α-*Pf*AMA1) or mouse monoclonal Ab against *Pf*RON4 (α-*Pf*RON4), then stained against *Pf*RON2, *Pf*AMA1, *Pf*RON4, or *Pf*RhopH2. $AMA1_{83}$ is a proprotein form and $AMA1_{66}$ is a processed form.

antibody, considering that these 3 proteins are distinct molecules that do not possess any similarity each other, this specific co-immunoprecipitation suggests complex formation among *Pf*RON2, *Pf*RON4, and *Pf*AMA1 in *P. falciparum*. The fact that both the 83-kDa proform and the 66-kDa processed form were co-precipitated with *Pf*RON2 indicated that a region responsible for complex formation was located in the 66-kDa form of AMA1 [30]. Neither of these was detected in the anti-RhopH2 immunoprecipitate, thereby excluding not only the possibility of *Pf*RON2 involvement in the RhopH complex, but also potential carryover due to insufficient or inadequate washing steps.

3.5. RON2 is expressed at the rhoptry neck of Plasmodium merozoites

Dual labeling indirect immunofluorescent assay was performed using anti-*Pf*RON2 with either anti-*Pf*AMA1 (microneme marker), anti-Clag3.1 (rhoptry body marker), or anti-*Pf*RON4 (rhoptry neck marker) antibodies in order to determine the sub-cellular location of *Pf*RON2 in *P. falciparum* (Fig. 6). In segmented schizonts, RON2 antisera produced a punctate pattern of fluorescence and each developing merozoite showed a single small punctate *Pf*RON2-positive signal located at the apical end. Although some parts of the *Pf*RON2 signal

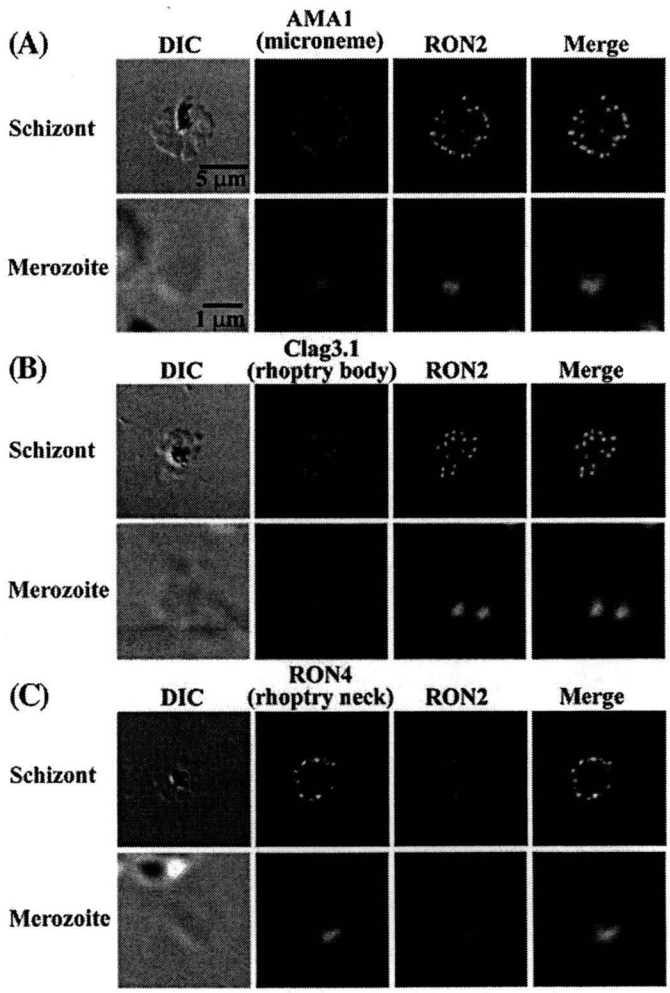

Fig. 6. *Pf*RON2 is expressed at the apical end of *Plasmodium* merozoites. Schizont-infected erythrocytes and merozoites were dual-labeled with antisera against *Pf*RON2 and *Pf*AMA1 (A), *Pf*Clag3.1 (B), or *Pf*RON4 (C). Merged images are shown in the right panels. All segmented schizonts and merozoites are positive for *Pf*RON2. Nuclei are counterstained with DAPI. Colocalization of *Pf*RON2 with *Pf*RON4 (rhoptry neck marker) was observed but neither colocalized with *Pf*Clag3.1 (rhoptry body marker) nor *Pf*AMA1 (microneme marker). To eliminate the background staining, negative control sera were always used and images were assessed (data not shown).

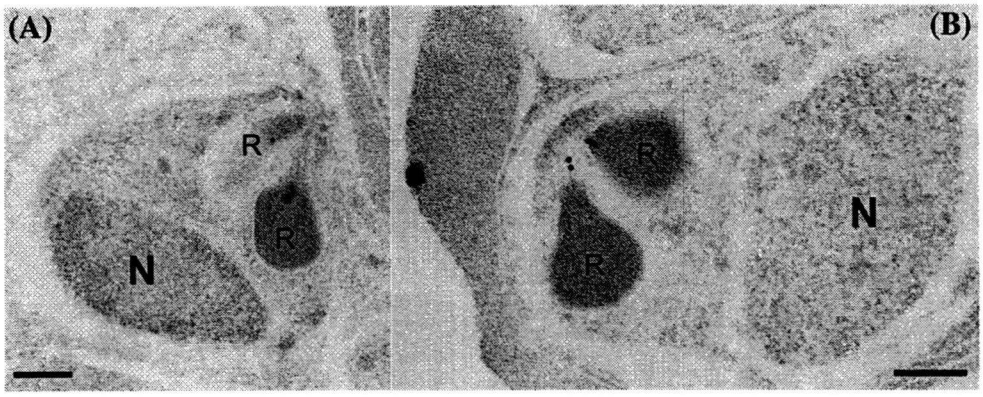

Fig. 7. Rhoptry neck localization of *Pf*RON2 by immunoelectron microscopy. Longitudinally sectioned merozoites in schizont-infected erythrocytes were labeled with anti-*Pf*RON2 serum followed by secondary Ab conjugated with gold particles. Gold particles were restricted to the narrow neck portion of the rhoptries (R). Two different images are shown (A and B). N indicates nucleus. Bars = 200 nm.

overlapped with microneme protein AMA1 and rhoptry body protein Clag3.1, it did not colocalize well with those markers, whereas complete colocalization was observed with the rhoptry neck marker *Pf*RON4.

Immunoelectron microscopy was carried out to determine the precise localization of the protein. *Pf*RON2 was detected in the neck portion of the pear-shaped rhoptries in segmented schizonts (Fig. 7). Thus *Pf*RON2 is seen to compartmentalize in the rhoptry neck.

3.6. Potential positive diversifying selection on *PfRON2*

To evaluate the polymorphic nature of *Pf*RON2, we sequenced the *pfron2* nucleotide sequence (2459–6570), excluding the 5′ low complexity region, in 5 *P. falciparum* parasite lines and compared them with the sequence from the genome database (3D7 line). A total of 5 nonsynonymous nucleotide substitutions were observed at nucleotide positions 2615, 2710, 2914, 4391 and 4392, resulting 4 amino acid substitutions (Table 1). An excess of nonsynonymous substitutions ($d_N = 0.0007 \pm 0.0003$) over synonymous substitutions ($d_S = 0.0002 \pm 0.0002$) was detected ($P = 0.0333$), indicating *Pf*RON2 is subject to positive diversifying selection.

4. Discussion

In this study, we characterized *P. falciparum* RON2 for its protein structure, transcription profiles, intracellular localization, and complex formation with *Pf*RON4 and *Pf*AMA1.

*Pf*RON2 possesses a region harboring homology with another rhoptry protein RhopH1/Clag, a component of the RhopH complex that possesses erythrocyte binding ability [16,31,32]. Co-immunoprecipitation showed that *Pf*RON2 does not form a complex with RhopH2, suggesting that *Pf*RON2 is unlikely to be a component of the RhopH complex. Because RON2 orthologs can be found in other apicomplexan parasites and RhopH1/Clag is found only in *Plasmodium* species, RhopH1/Clag probably evolved via acquisition of a conserved functional domain from RON2 during its generation in *Plasmodium* species. Thus, this homologous region may have a common function between these two complexes. The sequence of *Tg*RON2 deposited to the database (GenBank accession number DQ096563) only possesses the C-terminal half of the conserved region between RON2 and RhopH1/Clag. By comparing *Tg*RON2 gDNA and cDNA sequences, we noticed that intron 3 is relatively large (2272 bp) and contains a potential sequence encoding the N-terminal portion of the conserved region. Thus it is possible that there is another alternatively spliced transcript encoding the full length of the conserved region. Alternatively, it is also possible that this region represents an ancient vestigial exon.

Interestingly, we could readily detect complex formation between AMA1 and RON proteins in the extract obtained from mature schizont-rich parasites, suggesting that complex formation had already occurred at the schizont stage likely at the apical end upon secretion of RON proteins from rhoptry and AMA1 from microneme. This is in contrast to the other apicomplexa parasite *T. gondii*, in which the AMA1-RON complex was proposed to form at the initial contact with the host cell. The precise timing of the complex formation is not clear, but may vary depending on the parasite species. Among RON proteins characterized thus far, only *Tg*RON4 was visualized to locate at the moving junction during cell invasion. Whether *Pf*RON2 and *Pf*RON4 locate at the moving junction and whether the complex remains intact during cell invasion are still need to be clarified. We found that *Pf*RON2 degraded more rapidly than *Pf*RON4 after extraction (Fig. S4), which may explain the previous observation by Alexander et al. (2006), who did not detect *Pf*RON2 in the immunoprecipitant with anti-*Pf*AMA1 Ab [7].

The association between the 83-kDa proform of *Pf*AMA1 with RON proteins raises the possibility that the processing of *Pf*AMA1 from the 83-kDa form to 66-kDa form occurs not only in the microneme, as previously proposed [33], but also on the apical tip of the merozoite after release from the microneme in mature schizonts. If this is the case, it is not clear whether this AMA1 processing occurs after complex formation with RON proteins or is mainly achieved prior to this. However, it is formally possible that disruption of the different intracellular microorganelles during the experimental procedure resulted in an artificial complex formation of *Pf*AMA1 proform, for which further studies are required.

Due to the fact that *P. falciparum* AMA1 exhibits relatively high polymorphism between lines, which is considered to be generated by positive diversifying selection under the human immune pressure, we evaluated the polymorphic nature of *Pf*RON2. Although the level of polymorphism of RON2 is not high, the fact that $d_N > d_S$ suggests that positive diversifying selection does indeed act on RON2. Three types of

Table 1
Nucleotide and amino acid polymorphism of *Pf*RON2

Nucleotide positions (amino acid) [a]	Parasite line					
	3D7	7G8	HB3	Dd2	FVO	D10
2614–2616	tCa (Ser)	tCa (Ser)	tCa (Ser)	tCa (Ser)	tCa (Ser)	tTa (Leu)
2710–2712	Cat (His)	Cat (His)	Cat (His)	Tat (Tyr)	Tat (Tyr)	Tat (Tyr)
2914–2916	Gac (Asp)	Gac (Asp)	Cac (His)	Gac (Asp)	Gac (Asp)	Gac (Asp)
4390–4392	gAA (Glu)	gAA (Glu)	gAC (Asp)	gGC (Gly)	gGC (Gly)	gAA (Glu)

[a] Nucleotide numbering is after the 3D7 line sequence.

amino acid substitutions found at aa 1464 (Asp, Glu, and Gly) suggests that this particular site is under diversifying selection and is possibly to be exposed to host immunity. Thus, *Pf*RON2 not only appears to have an important role in host cell invasion by apicomplexan parasites, but also is a potential target for malaria intervention strategies.

Acknowledgements

We thank N Iyoku for her expertise, I Ling for anti-*Pf*RhopH2 serum, C Long for anti-*Pf*AMA1 serum, anti-*Pf*RON4 antibody (26C64F12) for J-F Dubremetz, and R Culleton for critical reading. Preliminary sequence data of *P. knowlesi*, *P. berghei*, *P. chabaudi*, and *B. bigemina* were produced by the corresponding groups at the Sanger Institute website at http://www.sanger.ac.uk/. Preliminary sequence data of *P. vivax* was produced at the Institute for Genomic Research website at http://www.tigr.org. This work was supported in part by Grants-in-Aid for Scientific Research 17590372 and 17406009 (to OK) from the Ministry of Education, Culture, Sports, Science and Technology, Japan. JC acknowledges the support of National Natural Science Foundation of China 30700695.

Appendix A. Supplementary data

Supplementary data associated with this article can be found, in the online version, at doi:10.1016/j.parint.2008.09.005.

References

[1] Snow RW, Guerra CA, Noor AM, Myint HY, Hay SI. The global distribution of clinical episodes of *Plasmodium falciparum* malaria. Nature 2005;434:214–7.
[2] Kaneko O. Erythrocyte invasion: vocabulary and grammar of the *Plasmodium* rhoptry. Parasitol Int 2007;56:255–62.
[3] Aikawa M, Miller LH, Johnson J, Rabbege J. Erythrocyte entry by malarial parasites. a moving junction between erythrocyte and parasite. J Cell Biol 1978;77:72–82.
[4] Boothroyd JC, Dubremetz JF. Kiss and spit: the dual roles of *Toxoplasma* rhoptries. Nat Rev Microbiol 2008;6:79–88.
[5] Alexander DL, Mital J, Ward GE, Bradley P, Boothroyd JC. Identification of the moving junction complex of *Toxoplasma gondii*: a collaboration between distinct secretory organelles. PLoS Pathog 2005;1:e17.
[6] Lebrun M, Michelin A, El Hajj H, Poncet J, Bradley PJ, Vial H, et al. The rhoptry neck protein RON4 re-localizes at the moving junction during *Toxoplasma gondii* invasion. Cell Microbiol 2005;7: 1823–33.
[7] Alexander DL, Arastu-Kapur S, Dubremetz JF, Boothroyd JC. *Plasmodium falciparum* AMA1 binds a rhoptry neck protein homologous to TgRON4, a component of the moving junction in *Toxoplasma gondii*. Eukaryot Cell 2006;5:1169–73.
[8] Baum J, Tonkin CJ, Paul AS, Rug M, Smith BJ, Gould SB, et al. A malaria parasite formin regulates actin polymerization and localizes to the parasite-erythrocyte moving junction during invasion. Cell Host Microbe 2008;3:188–98.
[9] Triglia T, Healer J, Caruana SR, Hodder AN, Anders RF, Crabb BS, et al. Apical membrane antigen 1 plays a central role in erythrocyte invasion by *Plasmodium* species. Mol Microbiol 2000;38:706–18.
[10] Hehl AB, Lekutis C, Grigg ME, Bradley PJ, Dubremetz JF, Ortega-Barria E, et al. *Toxoplasma gondii* homologue of *Plasmodium* apical membrane antigen 1 is involved in invasion of host cells. Infect Immun 2000;68:7078–86.
[11] Mital J, Meissner M, Soldati D, Ward GE. Conditional expression of *Toxoplasma gondii* apical membrane antigen-1 (TgAMA1) demonstrates that TgAMA1 plays a critical role in host cell invasion. Mol Biol Cell 2005;16:4341–9.
[12] Trager W, Jensen JB. Human malaria parasites in continuous culture. Science 1976;193:673–5.
[13] Bahl A, Brunk B, Crabtree J, Fraunholz MJ, Gajria B, Grant GR, et al. PlasmoDB: the *Plasmodium* genome resource. a database integrating experimental and computational data. Nucleic Acids Res 2003;31:212–5.
[14] Tsuboi T, Takeo S, Iriko H, Jin L, Tsuchimochi M, Matsuda S, et al. The wheat germ cell-free based production of malaria proteins for discovery of novel vaccine candidates. Infect Immun 2008;76:1702–8.
[15] Ling IT, Kaneko O, Narum DL, Tsuboi T, Howell S, Taylor HM, et al. Characterisation of the *rhoph2* gene of *Plasmodium falciparum* and *Plasmodium yoelii*. Mol Biochem Parasitol 2003;127:47–57.
[16] Kaneko O, Yim Lim BY, Iriko H, Ling IT, Otsuki H, Grainger M, et al. Apical expression of three RhopH1/Clag proteins as components of the *Plasmodium falciparum* RhopH complex. Mol Biochem Parasitol 2005;143:20–8.
[17] Kaneko O, Fidock DA, Schwartz OM, Miller LH. Disruption of the C-terminal region of EBA-175 in the Dd2/Nm clone of *Plasmodium falciparum* does not affect erythrocyte invasion. Mol Biochem Parasitol 2000;110:135–46.
[18] Torii M, Adams JH, Miller LH, Aikawa M. Release of merozoite dense granules during erythrocyte invasion by *Plasmodium knowlesi*. Infect Immun 1989;57: 3230–3.
[19] Aikawa M, Atkinson CT. Immunoelectron microscopy of parasites. Adv Parasitol 1990;29:151–214.
[20] Bendtsen JD, Nielsen H, von Heijne G, Brunak S. Improved prediction of signal peptides: signalP 3.0. J Mol Biol 2004;340:783–95.
[21] Hofmann K, Stoffel W. TMbase — a database of membrane spanning proteins segments. Biol Chem Hoppe-Seyler 1993;374:166.
[22] Krogh A, Larsson B, von Heijne G, Sonnhammer EL. Predicting transmembrane protein topology with a hidden Markov model: application to complete genomes. J Mol Biol 2001;305:567–80.
[23] Linding R, Russell RB, Neduva V, Gibson TJ. GlobPlot: exploring protein sequences for globularity and disorder. Nucleic Acids Res 2003;31:3701–8.
[24] Edgar RC. MUSCLE: multiple sequence alignment with high accuracy and high throughput. Nucleic Acids Res 2004;32:1792–7.
[25] Tamura K, Dudley J, Nei M, Kumar S. MEGA4: Molecular Evolutionary Genetics Analysis (MEGA) software version 4.0. Mol Biol Evol 2007;24:1596–9.
[26] Altschul SF, Madden TL, Schäffer AA, Zhang J, Zhang Z, Miller W, et al. Gapped BLAST and PSI-BLAST: a new generation of protein database search programs. Nucleic Acids Res 1997;25: 3389–402.
[27] Pain A, Renauld H, Berriman M, Murphy L, Yeats CA, Weir W, et al. Genome of the host-cell transforming parasite *Theileria annulata* compared with *T. parva*. Science 2005;309:131–3.
[28] Gardner MJ, Bishop R, Shah T, de Villiers EP, Carlton JM, Hall N, et al. Genome sequence of *Theileria parva*, a bovine pathogen that transforms lymphocytes. Science 2005;309:134–7.
[29] Le Roch KG, Zhou Y, Blair PL, Grainger M, Moch JK, Haynes JD, et al. Discovery of gene function by expression profiling of the malaria parasite life cycle. Science 2003;301:1503–8.
[30] Howell SA, Withers-Martinez C, Kocken CH, Thomas AW, Blackman MJ. Proteolytic processing and primary structure of *Plasmodium falciparum* apical membrane antigen-1. J Biol Chem 2001;276:31311–20.
[31] Ghoneim A, Kaneko O, Tsuboi T, Torii M. The *Plasmodium falciparum* RhopH2 promoter and first 24 amino acids are sufficient to target proteins to the rhoptries. Parasitol Int 2007;56:31–43.
[32] Rungruang T, Kaneko O, Murakami Y, Tsuboi T, Hamamoto H, Akimitsu N, et al. Erythrocyte surface glycosylphosphatidyl inositol anchored receptor for the malaria parasite. Mol Biochem Parasitol 2005;140:13–21.
[33] Healer J, Triglia T, Hodder AN, Gemmill AW, Cowman AF. Functional analysis of *Plasmodium falciparum* apical membrane antigen 1 utilizing interspecies domains. Infect Immun 2005;73:2444–51.

Parasitology International 58 (2009) 196–199

Contents lists available at ScienceDirect

Parasitology International

journal homepage: www.elsevier.com/locate/parint

Short communication

A small-scale systematic analysis of alternative splicing in *Plasmodium falciparum*

Hideyuki Iriko [a,b,c], Ling Jin [a,b], Osamu Kaneko [d,e], Satoru Takeo [b], Eun-Taek Han [b,f], Mayumi Tachibana [d], Hitoshi Otsuki [d], Motomi Torii [d], Takafumi Tsuboi [a,b,*]

[a] *Venture Business Laboratory, Ehime University, Matsuyama, Ehime 790-8577, Japan*
[b] *Cell-Free Science and Technology Research Center, Ehime University, Matsuyama, Ehime 790-8577, Japan*
[c] *Department of Microbiology and Pathology, Faculty of Medicine, Tottori University, Yonago, Tottori 683-8503, Japan*
[d] *Department of Molecular Parasitology, Ehime University Graduate School of Medicine, Toon, Ehime 791-0295, Japan*
[e] *Department of Protozoology, Institute of Tropical Medicine (NEKKEN), Nagasaki University, Sakamoto, Nagasaki 852-8523, Japan*
[f] *Department of Parasitology, Kangwon National University College of Medicine, Chunchon 200-701, Republic of Korea*

ARTICLE INFO

Article history:
Received 6 November 2008
Received in revised form 30 January 2009
Accepted 15 February 2009
Available online 5 March 2009

Keywords:
Alternative splicing
Exon definition
Gametocyte
Malaria
Plasmodium falciparum

ABSTRACT

During the last decade transcriptome analyses demonstrated that alternative splicing plays an important role to generate a large number of mRNA and protein isoforms from a limited number of genes. However, the frequency of the alternative splicing dramatically varies among living organisms. For example, 35–65% of human genes are involved in alternative splicing, whereas only a few are reported for unicellular organism yeast. Alternative splicing has been observed for several genes in the deadliest malaria parasite *Plasmodium falciparum*, but the frequency and the type were not systematically analyzed so far. In this study, we determined partial cDNA sequences for 88 open reading frames surrounding 246 introns in *P. falciparum* which were transcribed at schizont and gametocyte stages, and observed 15 instances of alternative splicing within a total of 14 gene transcripts, 16% of the analyzed genes. Among 5 basic splicing patterns, alternative 5′ and 3′ splicing, and intron retention were detected. Alternative splicing in 7 open reading frames had effects on the domain architectures of the gene products, which might result in modifying the cellular localization and function of these products.

Malaria is a significant human disease of global concern that causes several million deaths annually, as well as hundreds of millions of episodes of clinical illness. The intricate life cycle of the pathogenic protozoan agent of malaria, *Plasmodium*, belays an extraordinary biological complexity that underlies its development in both a warm-blooded host and mosquito vector. The parasite has the capacity to recognize and infect multiple cell types, such as salivary glands, hepatocytes, and erythrocytes; and has three distinct motile or invasive stages that traverse different tissues before infecting a new host cell [1]. In comparison to the simple unicellular yeasts, which are predicted to have ~5000 genes [2], the estimated size of the *Plasmodium* genome appears to inadequately reflect the remarkable biological complexity of its life cycle. The *Plasmodium falciparum* genome is estimated to have ~6000 genes, and the complexity of unique genes is considerably less due to the amplification of numerous multi-gene families, such as *var*, *rif*, and *stevor* [3], that occupy a significant part of the *Plasmodium* genome.

During the last decade transcriptome analyses demonstrated that alternative splicing plays an important role to generate a large number of mRNA and protein isoforms from a limited number of genes [4,5]. However, the frequency of the alternative splicing dramatically varies among living organisms. For example, 35–65% of human genes are involved in alternative splicing, whereas only a few are reported for yeast [4], despite the observation of 4730 predicted introns that are encoded within *Schizosaccharomyces pombe* genes [2]. In *P. falciparum*, 7406 introns were predicted in the genome, whereas alternative splicing has been observed only for a few genes that might affect protein function. For example, adenylyl cyclase variant isoforms may have functional differences [6]; and MAEBL variant isoforms are suggested to change the type I membrane product to a soluble isoform [7]. Another example is the stromal-processing peptidase and delta-aminolevulinic acid dehydratase, which share a common apicoplast-targeting leader sequence via the skipping of 4 intervening exons [8]. Alternative splicing was also reported for the blood stage antigen 41-3 precursor [9]; CDK-related protein kinase 6 [10]; and an aspartyl protease [11]. Thus, alternative splicing does occur in *Plasmodium*; however, the information is largely anecdotal and the prevalence of this mechanism remains unclear. Since alternative splicing can profoundly affect estimations of the breadth and complexity of the proteome (mRNA sequences) from the genome nucleotide sequence information, algorithms predictive of alternative splicing are increasingly needed. Indeed, we have observed in *P. falciparum* that alternatively spliced transcripts are not as rare as the anecdotal evidence would suggest, in the course of our experiences performing high-throughput cloning of protein expression constructs using cDNA templates [12]. In this report, we summarize our data and

Abbreviations: ORF, open reading frame.

* Corresponding author. Venture Business Laboratory, Ehime University, Matsuyama, Ehime 790-8577, Japan. Tel.: +81 89 927 8277; fax: +81 89 927 9941.
E-mail address: tsuboi@ccr.ehime-u.ac.jp (T. Tsuboi).

1383-5769/$ – see front matter © 2009 Elsevier Ireland Ltd. All rights reserved.
doi:10.1016/j.parint.2009.02.002

assess the frequency and the type of alternative splicing in *P. falciparum*; and predict the effect of altered transcripts on the localization and function of the produced proteins. Moreover, we provide evidence that the protozoan *P. falciparum* possesses both exon- and intron-recognition systems that initiate intron splicing.

The *P. falciparum* NF54 line was maintained in culture as described [13]. Asynchronous parasites were collected, and the erythrocytes were removed by saponin-mediated lysis. Parasite pellets were washed with phosphate buffered saline, and stored at −80 °C until use. Gametocyte stages were induced by maintaining parasite cultures at 37 °C using a gas mixture (90% N_2, 5% O_2, and 5% CO_2) for an extended period of time without the addition of fresh erythrocytes, and fully matured gametocytes were collected, washed in phosphate buffered saline, and stored at −80 °C until use. Sixty-nine % of the parasites were fully matured stage V gametocytes. Total RNA was extracted from parasite pellets using the RNeasy mini kit (Qiagen, Valencia, CA), and RNA preparations were extensively treated with DNase I to remove contaminating DNA. cDNA was prepared using Superscript III reverse-transcriptase (RT; Invitrogen, Carlsbad, CA). Open reading frames (ORFs) transcribed at schizont and gametocyte stages were selected for the analysis based on the transcriptome analysis [14]. Oligonucleotide primers were designed based upon annotated sequences in PlasmoDB [15], in order to PCR amplify predicted full-length ORFs. Eighty-eight ORFs were amplified by RT-PCR and cloned into the pCR2.1-TOPO TA plasmid (Invitrogen). Nucleotide sequence of the inserts were determined for 2 to 8 clones for each ORF using an ABI PRISM® 310 and 3100 Genetic Analyzers (Applied Biosystems, Foster City, CA) with M13(-20) and M13 reverse primers.

In this manner we randomly determined partial cDNA sequences for 88 ORFs surrounding 246 introns. The distribution of the ORFs arranged according to stage-specificity of the transcriptional cluster [14] and the number of the constituent introns are described in greater detail in Table 1. Similar to most other eukaryotes, exon boundaries of *Plasmodium* are demarcated by consensus donor and acceptor splicing junctions, GU and AG, respectively [16]. We observed 15 instances of alternative splicing within a total of 14 gene transcripts, 16% of the analyzed 88 genes (Table 1 and Supplementary Table 1). Because we only sequenced 2 to 8 clones for each intron, this value should be taken as a minimal estimation, and the true frequency of the alternative splicing is expected to be higher. To evaluate the alternative splicing in other strain, we performed RT-PCR analysis using gametocyte pellet purified from a malaria patient blood obtained from malaria endemic area in Mae Sot, Thailand. We checked 7 genes specifically expressed at gametocyte stage (PFE0220w, MAL8P1.149, MAL13P1.85, MAL13P1.211, PFD0700c, PF13_0220, and PFE0680w). As a result, five genes (PFE0220w, MAL8P1.149, MAL13P1.85, PFD0700c, and PF13_0220) also showed alternatively spliced variants together with the predicted parent transcripts as NF54 (data not shown). These results suggest that alternative splicing also occur in naturally isolated *P. falciparum* parasites. It was shown that alternative splicing in *P. falciparum* is a higher level than expected, based on the rarity of alternative splicing events in *S. pombe* [4].

The observed alternative splicing events were classified into 3 types: alternative 5′ splicing (46.7% of cases); alternative 3′ splicing (26.7% of cases); and intron retention/creation (26.7% of cases) (Fig. 1A). Notably, this is the first evidence of alternative 5′ splicing in *P. falciparum*. Another type of alternative splicing is exon skipping, which is the most prominent splicing pattern in metazoans; for example, 38% of events in humans are due to exon skipping [4,5]. Although 3 cases of exon skipping have been reported in *P. falciparum* [6,8,9], we did not observe this type occurring in this study.

Table 1
Analyzed *Plasmodium falciparum* introns in this study.

Cluster[a]	Stage[b]	Total		Alternative splicing	
		ORFs	Introns	ORFs (%)	Introns (%)
3	Gm	42	160	8 (19.0%)	9 (6.0%)
4	R/Sch/Mz	16	18	2 (12.5%)	2 (11.8%)
13	Sch/Gm	2	2	0 (0.0%)	0 (0.0%)
14	Spz/Sch/Gm	6	13	2 (33.3%)	2 (15.4%)
15	Sch	22	53	2 (9.1%)	2 (3.8%)
Total		88	246	14 (16.0%)	15 (6.4%)

[a] Open reading frames (ORF) were clustered based on the transcription pattern [14].
[b] Gm, gametocyte; R, ring; Sch, schizont; Mz, merozoite; Spz, sporozoite.

To assess the effect of the predicted alternative protein products, we analyzed the domain architectures of the splicing variants. Alternative splicing in 7 ORFs (MAL13P1.211, PFE0220w, PF13_0220, PF10_0021, PFD0700c, PF14_0694, and PFI0110c) had effects on the domain architectures of the gene products (Fig. 1B). The predicted parent transcripts (type 1) of MAL13P1.211 and PFE0220w encode proteins which possess a single transmembrane domain at their C-termini; whereas the alternatively spliced products harbored a frameshift and an early stop codon that resulted in truncated proteins lacking transmembrane domains. The cellular localization is therefore likely to depend on the splicing status, and the presence or absence of a transmembrane domain. Other transcripts (type 1) corresponding to PFD0700c, PF14_0694, and PFI0110c possessed at their C-termini an RNA recognition motif, thioredoxin motif, and protein kinase domain, respectively; whereas alternatively spliced variants (type 2) lacked these domains either partially or completely, suggesting that the protein functions would be abolished or suppressed. Although no known functional domains were detected for PF13_0220 or PF10_0021, the type 2 transcripts encode stop codons approximately 20 to 30 amino acids from the start codon, indicating that their expression as mature forms would be abolished.

Interestingly, among the two types of transcripts showing 5′ alternative splicing in *P. falciparum* the transcripts that encoded truncated product (type 2) almost always possessed a splicing site at the 5′ side compared to the predicted parent transcripts (type 1). This suggests that splicing site at 3′ side is original and that a cryptic splice site was activated in the preceding exon, likely weak splicing signal of the original site. In unicellular eukaryote yeast, mutations in splice sites lead to the activation of cryptic splice sites located downstream of the mutated site, suggesting that splicing machineries initially recognize intron (intron definition) [17]. However, in the metazoans, mutations in splice sites typically lead to the activation of cryptic splice sites located in the preceding exon or exon skipping [18], suggesting that the exon is primarily recognized (exon definition). Thus the pattern observed for *P. falciparum* fits to the "exon definition". Furthermore, 3 cases of exon skipping reported in *P. falciparum* support the presence of the "exon definition" system in this protist [6,8,9]. Because the observed intron retentions suggest the presence of "intron definition" system, *P. falciparum* appears to initiate splicing via both "exon definition" and "intron definition" systems. This is similar to the metazoan, *Drosophila melanogaster*, for which both intron retention and exon skipping have been observed [19,20].

In this study, we found frequent 5′ alternative splicing, however this type has never been reported in *P. falciparum* despite well over a decade of molecular cloning history of numerous *P. falciparum* genes. This might be explained by our cloning strategy to target gametocyte transcripts rather than asexual stage transcripts (Fig. 1). Because the *Plasmodium* female gametocyte was shown to translationally repress specific mRNA species by forming a complex in the cytoplasm to store mRNA for translation after fertilization [21], there might be a relation between these two observations via mRNA binding proteins. In all eukaryotes, splicing is mediated by a macromolecular spliceosome machinery that consists of small nuclear ribonucleoproteins (snRNPs) and non-snRNP splicing factors with RNA binding motif, including serine–arginine-rich (SR) proteins. Among SR proteins, SF2/ASF shows multiple functions, one of which is to affect alternative splice site selection by antagonizing other SR proteins, such as SC35 and SRp20 [22,23]. SF2/ASF is also reported to associate with ribosomes to stimulate translation [24]. Such concerted regulation of nuclear and

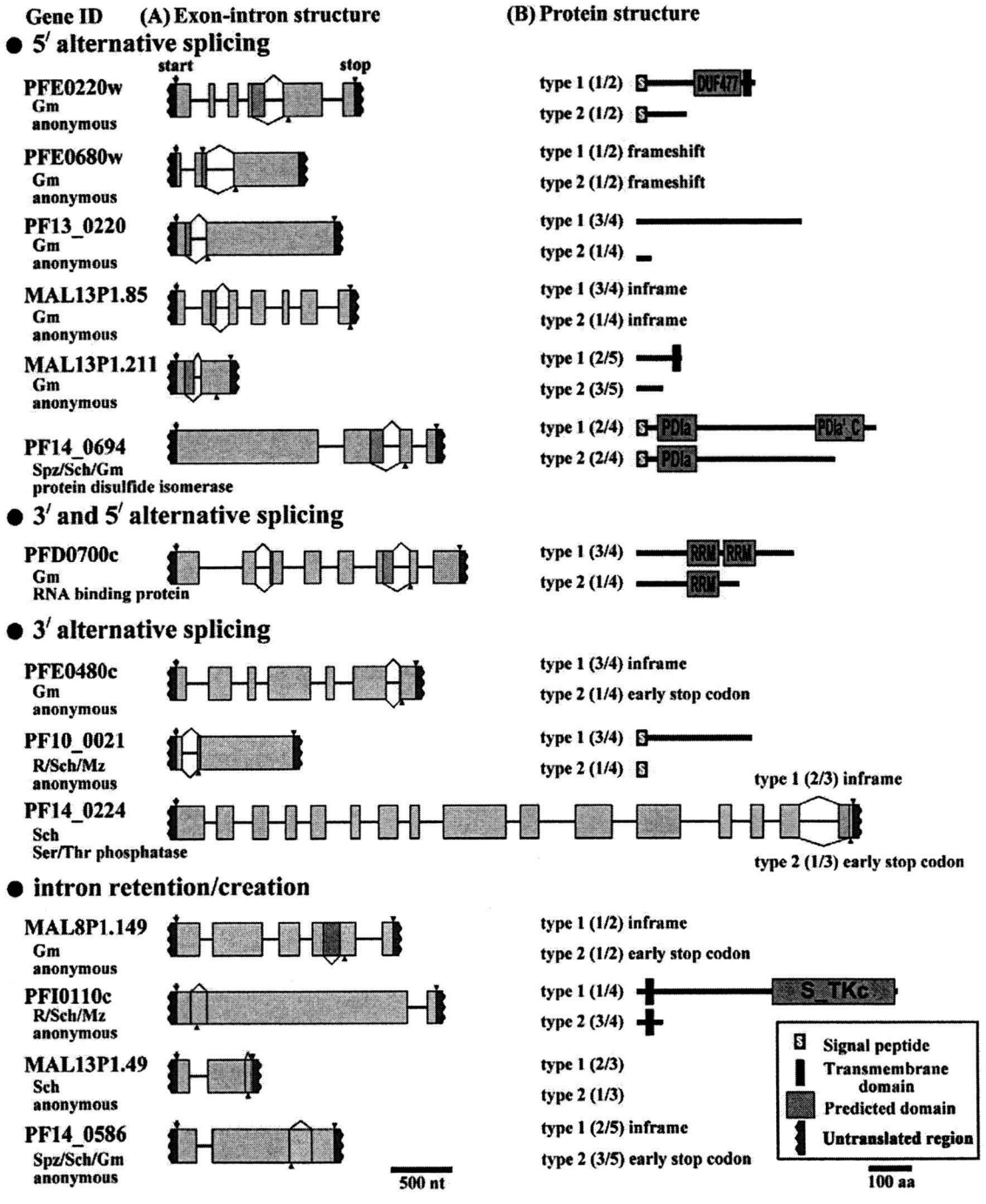

Fig. 1. Alternative splicing events that were detected in this study for *Plasmodium falciparum*. (A) Exon–intron boundaries for 2 types of transcripts are shown. Arrows indicate probable start codons. Arrowheads at the top or the bottom of each schematic indicate probable stop codons according to the exon–intron boundaries. Stage that transcribes each gene is shown under the Gene ID according to the transcriptome analysis [14]; Gm, gametocyte; Sch, schizont; R, ring; Mz, merozoite; Spz, sporozoite. Protein annotations refer to PlasmoDB [15]. (B) Predicted domain architectures of the proteins encoded by two variant transcripts. Type 1 is the presumed original transcript that encodes a longer open reading frame, whereas type 2 encodes a truncated product. The number of the clones for each type, per total clones, is shown in parentheses. Signal peptides and transmembrane domains were predicted by the SignalP and TMHMM2 programs, respectively. Domains were predicted by the SMART program (http://smart.embl-heidelberg.de/) or by searching the Conserved Domain Database (CDD) with Reverse Position Specific BLAST. Domains include: unknown function 477 (DUF477); thioredoxin domain of protein disulfide isomerase family (PDIa); C-terminal thioredoxin domain PDIa′ subfamily (PDIa′_C); Ser/Thr protein kinase motif (S_TKc); and the RNA recognition motif (RRM). The type of alternative splicing for the MAL8P1.149 is likely intron creation rather than intron retention, because type 1 possesses another intron and encoding longer open reading frame.

cytoplasmic activities of SR proteins was shown in mammalian cells [25]. A putative *P. falciparum* ortholog of SF2/ASF (PFE0865c and PF11_0205) might affect alternative splicing in *Plasmodium*. Interestingly, most of the *P. falciparum* genes reported to show alternative splicing are transcribed at the gametocyte and/or sporozoite stages [16], and this observation does not contradict our proposal.

In summary, among 88 isolated genes we found 14 genes that showed alternative splicing patterns, and half of these resulted in an alteration of the protein domain architecture. Splicing machinery initially recognized introns in *P. falciparum*, as suggested by the presence of intron retention, similar to the other unicellular eukaryote yeast. In addition, the pattern of alternative 5′ splicing, in combination with previous reports of the exon skipping, suggests that the exon is also recognized to initiate splicing in *P. falciparum*. This is an important observation, because unicellular eukaryotes are proposed to possess only an "intron definition" system, based on the data from yeast.